Out of the Mediterranean? Post-glacial colonisation pathways varied among cold-water coral species

Joana Ruela Heimbürger Boavida, Ronan Becheler, Marvin Choquet, Norbert Frank, Marco Taviani, Jean-François Bourillet, Anne-Leila Meistertzheim, Anthony Grehan, Alessandra Savini, Sophie Arnaud-Haond

Journal of Biogeography

Out of the Mediterranean? Post-glacial colonisation pathways varied among cold-water coral species

Journal:	*Journal of Biogeography*
Manuscript ID	JBI-18-0133.R1
Manuscript Type:	Research Paper
Date Submitted by the Author:	n/a
Complete List of Authors:	boavida, joana; Ifremer Centre de Mediterranee, MARBEC; Centro de Ciencias do Mar, Biogeography Ecology and Evolution Lab Becheler, Ronan; Ifremer Centre de Mediterranee, MARBEC; UPMC Univ Paris 6, CNRS, UMI 3614 Evolutionary Biology and Ecology of Algae, Sorbonne Université; Station Biologique de Roscoff, Station Biologique de Roscoff Choquet, Marvin; Ifremer Centre de Mediterranee, MARBEC; Nord University, Faculty of Biosciences and Aquaculture Frank, Norbert; Heidelberg University, Institute of Environmental Physics Taviani, Marco; Institute of Marine Science - National Research Council ISMAR-CNR, Institute of Marine Science - National Research Council ISMAR-CNR; Woods Hole Oceanographic Institution, Biology Department; Stazione Zoologica Anton Dohrn, Stazione Zoologica Anton Dohrn Bourillet, Jean Francois ; ifremer, Physical resources and sea floor ecosystems Department Meistertzheim, Anne Leila; Sorbonne Universités, Laboratoire d'Ecogéochimie des Environnements Benthiques (LECOB), Observatoire Océanologique de Banyuls Grehan, Anthony; NUI Galway, NUI Savini, Alessandra; Università degli Studi di Milano-Bicocca, Dept. of Earth and Environmental Sciences Arnaud-Haond, Sophie; Ifremer Centre de Mediterranee, MARBEC
Key Words:	Cold-water corals, Lophelia pertusa, Madrepora oculata, Marine phylogeography, Deep-sea, Last Glacial Maximum, Glacial marine refugia

i. Out of the Mediterranean? Post-glacial colonisation pathways varied among cold-water coral species

ii. Running title: Contrasting deep corals recolonisation paths

iii. Joana Ruela Heimbürger Boavida[1*±], Ronan Becheler[1,2,3,*§], Marvin Choquet[1,4], Norbert Frank[5], Marco Taviani[6,7,8], Jean-François Bourillet[9], Anne Leila Meistertzheim[10], Anthony Grehan[11], Alessandra Savini[12], Sophie Arnaud-Haond[1]

*Equal contribution

Correspondance: Joana Boavida Institut Français de Recherche pour l'Exploitation de la Mer, Marine Biodiversity Exploitation and Conservation - Marbec, Station de Sète - Avenue Jean Monnet - CS 30171, 34203 Sète Cedex, France

joanarboavida@gmail.com | +33 7 69 41 12 79

iv. The author's institutional affiliations

[1] Institut Français de Recherche pour l'Exploitation de la Mer, Marine Biodiversity Exploitation and Conservation - Marbec, Station de Sète - Avenue Jean Monnet - CS 30171, 34203 Sète Cedex, France

[2] CNRS, UMI 3614 Evolutionary Biology and Ecology of Algae, Sorbonne Université, UPMC Univ Paris 6

[3] Station Biologique de Roscoff, CS 90074, Place Georges Teissier, 29688 Roscoff cedex, France.

[4] Faculty of Biosciences and Aquaculture, Nord University, Bodø, Norway

[5] Heidelberg University, Institute of Environmental Physics, Im Neuenheimer Feld 229, 69120 Heidelberg, Germany

[6] Institute of Marine Science - National Research Council ISMAR-CNR, Via Gobetti 101, 40129 Bologna, Italy

[7] Biology Department, Woods Hole Oceanographic Institution, 266 Woods Hole Road, Woods Hole, MA 02543, USA

[8] Stazione Zoologica Anton Dohrn, Villa Comunale, 80121 Naples, Italy

[9] Institut Français de Recherche pour L'Exploitation de la Mer, Physical resources and sea floor ecosystems Department, Centre de Brest BP 70, F-29280, Brest - France

[10] Sorbonne Universités, CNRS, UPMC Univ Paris 06, Laboratoire d'Ecogéochimie des Environnements Benthiques (LECOB), Observatoire Océanologique de Banyuls, Banyuls sur mer, France

[11] Dept. of Earth & Ocean Sciences, Quadrangle Bldg, NUI Galway, Ireland

[12] Università degli Studi di Milano-Bicocca, Dept. of Earth and Environmental Sciences, Italy

§ Present address: Centro de Conservación Marina, Departamento de Ecología, Facultad de Ciencias Biológicas, Pontificia Universidad Católica de Chile, Casilla 114-D, Chile

± Present address: Centro de Ciências do Mar, Universidade do Algarve, Campus de Gambelas, 8005-139 Faro, Portugal

v. Acknowledgements

We are thankful to the teams involved in multiple oceanographic cruises: EU CoralFish's: ROV team, captain and crew of BOBECO, IceCTD, and CE98. We thank Franck Lartaud and Nadine Le Bris (chair 'Extreme environment, biodiversity and global change' Fondation TOTAL and UPMC; Coord.: N. Le Bris) for providing Mediterranean samples. Thanks to Lars-Eric Heimbürger for english edits. JB was supported by the European Union's H2020 research and innovation program under grant agreement Number: 678760 (ATLAS). This work is a contribution to the European Union's FP7 and Horizon 2020 projects, respectively CoralFISH (under grant agreement no. 213144) and ATLAS (under grant agreement no. 678760), samples from the Adriatic Sea through the EU Coconet program. This is Ismar-CNR, Bologna scientific contribution n. 1960. This contribution reflects the authors' views and the European Union is not responsible for any use that may be made of the information it contains.

vi. Abstract and keywords:

Aim. To infer cold-water corals post-glacial phylogeography and assess the role of Mediterranean Sea glacial refugia as the origin for the recolonisation of the North-eastern Atlantic Ocean.

Location. North-eastern Atlantic Ocean and Mediterranean Sea.

Taxon. *Lophelia pertusa, Madrepora oculata.*

Methods. We sampled cold-water corals using remotely operated vehicles and performed one geological corer for coral and sediment dating. We characterized spatial genetic patterns (microsatellites and a nuclear gene fragment) using networks, clustering and measures of genetic differentiation.

Results. Microsatellite and sequence data were congruent, and showed a contrast between the two cold-water coral species. Populations of *L. pertusa* are not genetically structured across the North-eastern Atlantic, present a dominant pioneer haplotype, local haplotype radiations and a majority of endemic variation in lower latitudes. *M. oculata* populations are differentiated across the North-eastern Atlantic, and genetic lineages are poorly admixed even along neighbouring sites.

Conclusions. Our study shows contrasting post-glacial colonisation pathways for two key habitat-forming species in the deep-sea. The cold-water coral *L. pertusa* has likely undertaken a long-range (post-glacial) recolonisation of the North-eastern Atlantic directly from refugia located along southern Europe (Mediterranean Sea or Gulf of Cadiz). Contrastingly, the stronger genetic differentiation of *M. oculata* populations mirrors the effects of long-term isolation in multiple refugia. We suggest that the distinct and genetically diverged, refugial populations initiated the post-glacial recolonisation of North-eastern Atlantic margins, leading to a secondary contact in the northern range and reaching higher latitudes much later, in the late Holocene. This study highlights the need to disentangle the influence of present day dispersal and evolutionary processes on the distribution of genetic polymorphism, to unravel the influence of past and future environmental changes on connectivity in the cosmopolitan deep-sea ecosystems associated to cold-water corals. Marine phylogeography, Deep-sea, Cold-water corals, Last Glacial Maximum, *Lophelia pertusa*, *Madrepora oculata*, Glacial marine refugia

vii. Main text

Introduction

Cold-water corals (CWC) are amongst the most charismatic marine ecosystems in the deep ocean (>200 m), supporting abundant and diverse biomass (Milligan *et al.*, 2016). Deep-reef habitats rely upon the frame-building capability of several coral species, notably *Lophelia pertusa* and *Madrepora oculata* (Linnaeus, 1758). The two species intermingle and anastomose in reefs in the North-eastern Atlantic Ocean (NE Atlantic; Arnaud-Haond *et al.*, 2017). Yet, ever rising anthropogenic pressures in the deep-sea, like fisheries (Pusceddu *et al.*, 2014), oil and gas exploitation (Cordes *et al.*, 2016) and deep-sea mining (Wedding *et al.*, 2015), threaten vulnerable CWC. Protection of key deep-sea ecosystems is, therefore, an urgent priority, particularly in the face of global change, and strategic Marine Protected Areas, thoroughly assessed for their genetic connectivity, need to be established. Nonetheless, obtaining sufficient specimens and applying statistically robust sampling designs for genetic studies in the deep-sea remain challenging (Becheler *et al.*, 2017). While CWC connectivity has been assessed along the North Atlantic Ocean at the local and regional scale (LeGoff-Vitry *et al.*, 2004; Morrison *et al.*, 2011; Dahl *et al.*, 2012; Becheler *et al.*, 2017), effective conservation warrants information at the NE Atlantic basin scale (Fenberg *et al.*, 2012). Spatial distribution analyses of genetic diversity can be used to detect connectivity pathways across reefs, and to define key areas for the conservation of biodiversity.

Similarly, the present-day geographic distribution of many terrestrial and marine species and their genetic diversity is influenced by environmental gradients, contemporary dispersal and recent climatic events, notably the Last Glacial Maximum, LGM, (26 - 19 ka; Hewitt, 1996, 1999, 2004; Petit *et al.*, 2003; Maggs *et al.*, 2008; Clark, 2009). Repeated Pleistocene glaciations are known to impact deep-sea ecosystems (Bouchet & Taviani, 1992; Sabelli & Taviani, 2014; Vertino et al., 2014). However, their impact on CWC in particular remains understudied. Deep-sea species may not respond similarly to coastal species, because biological assemblages, environmental gradients and dispersal patterns are fundamentally different among ecosystems and geographical areas (Kousteni *et al.*, 2015; Shum *et al.*, 2015).

The biogeographic connectivity between Mediterranean and NE Atlantic CWC during and after the Pleistocene (ca. 2.7 Ma to 12 ka) glacial events can partially be inferred from paleo-records (Supplementary Paleo-history). While CWC have maintained a continuous presence in the Mediterranean Sea at least since the early Pleistocene (Vertino *et al.*, 2014), CWC in the NE Atlantic may have been more affected, with consequent local demise during the LGM (Frank *et al.*, 2011). Notably, the last cold oscillation, during the Younger Dryas (12.9-11.7 ka), represented a favourable period for CWC reef growth in the western Mediterranean Sea as well as in adjacent Atlantic regions at the Gulf of Cadiz and African margins (Schröder-Ritzrau et al., 2005; McCulloch et al., 2010; Taviani et al., 2011b). In contrast, growth episodes of CWC in the NE Atlantic have been restricted to warm climate stages and coral fossils are absent from strata corresponding to glacial episodes (Frank et al., 2009). Radiometric dating shows that NE Atlantic CWC are younger than the ones from the Mediterranean Sea, with ages estimated to be post-LGM (under 12,000 years; Freiwald & Roberts, 2005; Schröder-Ritzrau et al., 2005), producing a NE Atlantic CWC age-gradient from south to north (summarized in Fig. 1). Given such persistent occurrence of CWC, it has been argued that the Mediterranean basin may have acted as a CWC glacial refugium during range contractions in the North Atlantic Ocean during Pleistocene glaciations (De Mol *et al.*, 2002; Henry *et al.*, 2014). Such a refugium may have constituted the source for the Atlantic northward recolonisation of CWC at the end of the LGM by larvae, transported with intense flows of Mediterranean Outflow Water (MOW) since 50 ka (Fig. 1; Voelker *et al.*, 2006; Stumpf *et al.*, 2010).

Sympatric paleo-coral occurrence suggests a common history in terms of range contraction and expansion for *Lophelia pertusa* and *Madrepora oculata.* Such a common response to past-environmental change may not hold true in light of recent studies (Lartaud *et al.*, 2014, 2017) pointing to physiological differences between both species, particularly in terms of optimal growth temperatures. Dissimilar ecological strategies between the two CWC are possible. *Lophelia pertusa* presents potential for widespread larval dispersal (Strömberg and Larsson, 2017), high fecundity (Waller & Tyler, 2005) and a variable microbiome composition (Meistertzheim *et al.*, 2016). *Madrepora oculata* presents a different reproductive strategy, having much lower fecundity (Waller & Tyler, 2005) and a resilient microbiome (Meistertzheim *et al.*, 2016; and unknown larval characteristics). Although reduced genetic connectivity has been demonstrated for *L. pertusa* at an inter-basin scale along with moderate to high gene flow within regions (Morrison *et al.*, 2011; Dahl *et al.*, 2012; Flot *et al.*, 2013), the extent of CWC connectivity along the European margins and the role that extant populations had in the past remain to be tested. Here we investigate the population genetic diversity and structure of *L. pertusa* and *M. oculata* along the deep margins of the NE Atlantic, using nuclear data (microsatellites and sequences). We discuss how past environmental variations related to the LGM may have affected genetic diversity and structure of the two CWC species across this wide geographic region. We hypothesise that distinct ecological requirements in the deep-sea influence population structure and the distribution of genetic diversity within species. In particular, we expected that *L. pertusa* would present low levels of population differentiation across the NE Atlantic margins, consistent with a post-LGM northward expansion from southern refugia, and maintained by present-day connectivity. We expected *M. oculata* to present stronger population differentiation, consistent with lower fecundity. To these aims, we examined the genetic structure and diversity of *L. pertusa* and *M. oculata* within and among the principal biogeographic provinces of the NE Atlantic and the Mediterranean Sea where CWC are known to occur.

2. Materials and methods

2.1 Field collections

Two-hundred and seventy samples of *Lophelia pertusa* and 260 of *Madrepora oculata* were collected from six regions between 250 and 1,170 m-depth: the eastern Mediterranean basin (Ionian Sea, south-eastern Adriatic Sea); western Mediterranean basin (Gulf of Lions); Mid-Atlantic region (Azores); Bay of Biscay; Rockall Bank (off western Ireland); and the High latitudes (Iceland) (Fig. 1; Appendix Table S1). In one canyon of the Bay of Biscay, Petite Sole, two sample collections were made at different sections of the canyon. Samples were stored in 96% ethanol and stored frozen at -20 or -80°C prior to DNA extraction. *Lophelia pertusa* DNA was extracted aboard using the Fast DNA®SPIN for soil kit, according to the manufacturer protocol (MP Biomedicals, France); for *M. oculata* we used cetyl trimethyl ammonium bromide (Doyle & Doyle, 1988).

2.2 Core collection and dating

Within the Guilvinec Canyon (Bay of Biscay), a 1.2 m-length sediment core (BBCO-CS01) was collected (N46°56,045'; W005°21,642') at 815 m-depth. The core is representative of the superficial layers of the Armorican margin. Remains of coral skeleton were dated using the U/Th method at the Institute for Environmental Physics at Heidelberg University (Schröder-Ritzrau et al., 2003). Foraminifera from nearby sediments were ^{14}C-dated. Corals and foraminifera were subsequently calibrated to absolute ages using Intcal13 (Reimer et al., 2013).

2.3 DNA amplification and sequencing

The Internal Transcribed Spacer (ITS) ribosomal sequence was amplified using primers developed by Diekmann *et al.* (2001). ITS-sequences (262 samples of *L. pertusa* 1130 base pair, bp, 200 samples of

M. oculata 1124 bp) were proof-read and aligned using GENEIOUS v6.1 (Kearse *et al.*, 2012). Nine *L. pertusa* (Morrison *et al.*, 2008; Becheler *et al.*, 2017) and six *M. oculata* microsatellite markers were amplified following Becheler *et al.* (2017). Products were scored using GENEIOUS v5.6.4. One *L. pertusa* locus was discarded due to high frequency of null alleles (>30%). Clones were removed from each dataset (ITS and microsatellites). Statistical power was assessed for the two coral species (Appendix Supplementary methods S2). Only sites with five or more samples were kept for analyses.

2.4 Phylogeographic patterns and genetic diversity

Population genetic differentiation for ITS-sequences was assessed with pairwise haplotype F_{ST}-statistic (Weir & Cockerham, 1984) in ARLEQUIN v3 (Excoffier *et al.*, 2005). The distribution of genetic variability within and among groups was estimated with an Analysis of Molecular Variance (AMOVA) with ARLEQUIN on four groups for *L. pertusa*, and five for *M. oculata* (1. Mediterranean, 2. Bay of Biscay, 3. Rockall Bank and 4. High Latitudes, and 5. Mid Atlantic). Population genetic diversity was estimated with: i. the number of distinct and private haplotypes, ii. number of polymorphic sites, iii. haplotypic diversity (Nei, 1987), and iv. the mean number of pairwise differences (Tajima, 1983). Haplotype relationships were visualized with statistical parsimony networks,on TCS v1.21 (Clement *et al.*, 2000)

Microsatellite genetic diversity and structure were estimated with GENETIX v4.05 (Belkhir K., Borsa P., Chikhi L., 2004). The mean number of alleles per locus standardized to the lowest number of samples collected; estimates of observed (H_O) and unbiased (H_E) multi-locus heterozygosity (Nei, 1978); the F_{IS}-statistic and its significance (tested with 1000 permutations); and linkage disequilibrium, assessed through the index $\bar{r}_d$ with MULTILOCUS v1.3 (http://www.bio.ic.ac.uk/evolve/software/multilocus/) were calculated. Genetic structure (pairwise F_{ST}) was estimated with θ (Weir & Cockerham, 1984). Inference of spatial population structure with Bayesian clustering was done with TESS v2.3 (François *et al.*, 2006; Chen *et al.*, 2007) via the *tess3r* R package (The R Foundation for Statistical Computing, 2018).

We used Discriminant Analysis of Principle Components (DAPC; Jombart et al., 2010) implemented in the R package *adegenet* (Jombart, 2008), to determine whether the genotypes of *L. pertusa* and *M. oculata* were distinct between different sampling sites. We used k-means clustering (k=2 to maximum number of sampling sites) with the Bayesian Information Criterion (BIC) to identify an optimal number of genetic clusters that describe the data, as well as the α-score optimisation procedure to identify the optimal number of principal components (PCs) to retain (retaining too many PCs can lead to overfitting the discriminant functions). The α-score optimisation showed that approximately 25 PCs needed to be retained for *M. oculata* (>69.3% of the total variance), and 60 PCs for *L. pertusa* (28.9%). Next we used DAPC to derive membership probabilities for each individual in each of the groups using location priors (see Appendix Supplementary methods S2).

2.5 Demographic inferences

Historical fluctuations in population size for each sampled site were detected using Fu's Fs (Fu, 1996) and Tajima's D (Tajima, 1989) on ITS data from *L. pertusa* and *M. oculata*. Departures from mutation-drift equilibrium were tested under the null hypothesis of no significant change of effective population size, with ARLEQUIN. A negative value significantly different from constant population size is interpreted as a signature of population expansion; the significance of Fs and D values was determined by randomization.

The evolutionary and demographic histories of NE Atlantic and Mediterranean CWC (*L. pertusa* and *M. oculata*) were further reconstructed using Approximate Bayesian Computations (ABC) as implemented in DIYABC v2.1.0 (Cornuet et al., 2014). We used microsatellite and ITS sequence data for *M. oculata* and microsatellite only for *L. pertusa*. *Lophelia pertusa* populations were grouped according to the microsatellite Bayesian clustering (cluster 1 - Eastern Mediterranean, cluster 2 - Western Mediterranean, cluster 3 - Bay of Biscay and High latitudes, cluster 4 - Rockall bank) and for

M. oculata we used the geography-based population grouping. We compared competing scenarios in order to identify the patterns of post-LGM CWC range expansion along the NE Atlantic margins. Scenarios 1, 2 and 4 determine the pattern of colonisation of the northern edge of the NE Atlantic range, comparing models of stepping-stone colonization from the Mediterranean Sea to the Bay of Biscay and then further north (Scenario 1 - Stepwise range expansion), and models of admixture: between the Bay of Biscay, High latitudes and the west Mediterranean to produce the Rockall bank population (Scenario 2), between the High latitudes and Rockall bank to produce the Mid Atlantic population (Scenario 2 *M. oculata*), between the Bay of Biscay and Rockall bank to produce the Mid Atlantic population (Scenario 4 *M. oculata*), and between the Mediterranean Sea and the Bay of Biscay to produce the Mid Atlantic population (Scenario 5 *M. oculata*). Scenario 3 examined the demographic history of the NE Atlantic and Mediterranean populations with changes in population size since colonisation. We compared a null model of no change in population size (Scenarios 1 and 2) to a model of a short bottleneck (10 generations) during colonisation followed by population expansion (Scenario 3). In this scenario, at each split, there is an initial reduction of the population size of the newly formed population, because the expansion is assumed to start with few immigrants. For *L. pertusa* we used the known time of Rockall bank colonisation (approx. 9 ka; Frank et al., 2009) to calibrate divergence times (mode and 95% confidence interval) from the estimated ABC number of generations; we then assumed the same generation time (est. approx. 3 years) for *M. oculata*.

We generated 3 to $5x10^6$ simulations for each scenario tested using the combined microsatellite and ITS datasets for *M. oculata* and the microsatellite dataset for *L. pertusa* (Appendix Supplementary methods S2) to produce a set of pseudo-observed datasets (PODs). Effective population sizes and parameters for the Generalized Stepwise Mutation and Kimura two parameter models were set to default values, while time of population divergence (in generations) was defined as uniform within post-LGM periods (for model parameters see Appendix S2). The posterior probability of each scenario was inferred with a logistic regression performed on the 1% of PODs closest to the empirical data. We empirically evaluated the power of the model to discriminate among scenarios using a Monte Carlo estimation of false allocation rates (type1 and 2 errors) resulting from ABC posterior probabilities-based model selection.

Supplementary methods can be found in the Appendix (S2).

3. Results

3.1 Core collection and dating

Fossils of *Lophelia pertusa* and *Madrepora oculata* were found in the gravity core. The dating of CWC remains revealed ages ranging from present to 6,959 ± 169 years (U/Th corrected age).

3.2 Phylogeographic patterns and genetic diversity

Lophelia pertusa showed four genetically distinct groups: the eastern and the western Mediterranean Sea, the Rockall bank and the remaining NE Atlantic populations (Bay of Biscay and High latitudes) (Fig. 2a right). Within *L. pertusa*, the Mediterranean genetic ancestry, and in particular the west Mediterranean ancestry (blue) can be seen in low proportions across all NE Atlantic sites. The green genetic ancestry is maximized in Bay of Biscay and High latitudes populations, while the grey genetic ancestry (found in the Bay of Biscay and High latitudes sites) is maximized in the Rockall bank population. The grey ancestry component is present in high proportion in the High latitudes populations, particularly in Hafadsjup (HAF), which comprises over half of *L. pertusa* ancestry. Genetic differentiation was strong between east and west Mediterranean populations and weak across the NE Atlantic samples, with nearly all values not significantly different from zero. The Rockall bank population was differentiated from over half of the Bay of Biscay locations but not with the High latitudes populations (Appendix Table S4.1). Clustering analyses showed that *M. oculata* was also structured in four genetic clusters, but with a different organisation (Fig. 2a). The Mediterranean Sea and the High Latitudes formed two distinct clusters (displayed in red and grey on Fig. 2a left). The next two clusters are not so geographically coherent: The Bay of Biscay genetic ancestry (blue; third

cluster) is nearly absent from the Lampaul canyon, as well as from the Rockall bank and Mid Atlantic populations (which together form the fourth cluster). *M. oculata* populations from the Bay of Biscay harbour a strong Mediterranean genetic component (red) maximized in the northern Bay of Biscay canyons (Morgat, Crozon and Petite Sole), which is absent from most individuals in the Mid Atlantic, Lampaul canyon (in the Bay of Biscay) and Rockall bank populations. The NE Atlantic genetic ancestry (green) is well represented in all NE Atlantic populations and in smaller proportion in some Mediterranean individuals. The High latitudes genetic ancestry (grey) is found in high proportion in Rockall and Mid Atlantic populations. Mean pairwise F_{ST} between regions was high, up to 0.5 between the eastern Mediterranean Sea and the High Latitudes, but not significantly different from zero between eastern and western Mediterranean Sea populations, while nearly all pairwise F_{ST} values were significantly different from zero. Lack of population differentiation was observed between two Bay of Biscay canyons (CRZ-LMP), within one canyon (PS1-PS2), between High latitudes locations, and between Rockall bank and its closest High latitudes site, Londsjup (Appendix Table S4.2). Regional F_{ST} was significantly different from zero for all pairwise comparisons for the two coral species: Mediterranean Sea, Mid-Atlantic, Bay of Biscay, Rockall bank and High latitudes. The lowest regional F_{ST} for *M. oculata* was between the High latitudes and Rockall bank populations (0.051) and for *L. pertusa* between the High latitudes and Bay of Biscay populations (0.004).

The genetic affinities of the sampled individual corals were projected onto principal components (DAPC). As expected, the first axis of *L. pertusa* separates Mediterranean and NE Atlantic populations. Within each group, genetic variability is spread across the second axis: The Eastern Mediterranean samples at one end and the Western Mediterranean samples at the other end, a separation that is also clearly visible in the group membership probabilities on the bottom of figure 3b. The NE Atlantic genetic group along PC2 spans samples from the Bay of Biscay to the High latitudes, including Rockall bank (Fig. 3b). The most important *M. oculata* genetic affinities show a cline on the first axis, spanning samples from the lower (Mediterranean) to the higher latitudes. The gradient is visible in the group membership proportions shown on the bottom of figure 3a, particularly along the Bay of Biscay canyons and along Rockall-High latitudes populations.

Gene diversity and the average number of alleles per locus for *L. pertusa* and *M. oculata* samples were high (*L. pertusa* H_E 0.90 +/- 0.08, and 30.4 alleles per locus; *M. oculata* H_E 0.53 +/- 0.23 and 12.3 alleles per locus; Tables 1 and 2). Regionally, average allelic richness was higher at intermediate latitudes for both species (Mediterranean 7 for *L. pertusa* and 3 for *M. oculata*, Bay of Biscay 16 and 5, Rockall Bank 15 and 6, and High Latitudes 12 and 4, for *L. pertusa* and *M. oculata* respectively, and Mid Atlantic, where only *M. oculata* was sampled, 3). Private alleles were present in all sampled *L. pertusa* sites, while they were rarely present in *M. oculata* populations. *Madrepora oculata* presented higher private allelic richness in the Mediterranean basin (2-4). An excess of homozygotes was observed in all *L. pertusa* populations and in half of the *M. oculata* sites, particularly along the NE Atlantic populations.

The patterns of genetic structure inferred with ITS were generally concordant with those of microsatellites. Based on statistic parsimony, a haplotype network was constructed for *L. pertusa*, with one main ITS lineage inferred as the most likely ancestral haplotype (from a total of 39 haplotypes), which possibly radiated from lower to higher latitudes (>60% of samples), and many rare haplotypes (over 20 unique). The ancestral haplotype is nearly absent from Rockall bank *L. pertusa*, supporting the Bayesian clustering, where High latitudes and Bay of Biscay share a genetic ancestry (green) almost absent from Rockall bank samples. Two other well-represented haplotypes were restricted to: i) the Bay of Biscay, High Latitudes and Mediterranean Sea, and ii) mostly the Rockall Bank with few Bay of Biscay samples (Fig. 2b), supporting the Rockall bank genetic ancestry (grey) as distinct from relatively close populations (Bay of Biscay and High latitudes). The Atlantic sites harbour the majority of sequence variation. The Bay of Biscay has the highest number of haplotypes (24), with 12 haplotypes unique to this region, but the highest haplotype diversity (H=0.7) was found in the west Mediterranean Sea (Table 3). Ten haplotypes were observed in the Mediterranean Sea with two unique to the western Mediterranean. Iceland, regardless of the high latitude and recent CWC fossil ages (8.3 Ka, Fig. 1), harbours the second highest number of *L. pertusa* haplotypes (14; Appendix Table S7),

with two haplotypes exclusive to its CWC reefs. *L. pertusa* haplotypes are not particularly clustered and, except for the inferred ancestral haplotype, most haplotypes are found in moderate to low frequency at each site (Appendix Table S7). There are no *L. pertusa* region-specific haplotypes in the Bay of Biscay or the west Mediterranean Sea.

There was some phylogeographic clustering for the *M. oculata* haplotype network, with one lineage dominant in the Higher latitudes and Rockall bank, modestly present in distant, southern, geographic locations (e.g., one samples from the Mediterranean Sea), and absent from the Bay of Biscay. A quarter of all haplotypes are shared across distant geographic regions (i.e. High Latitudes and Mediterranean Sea). Haplotypes found in Mid-Atlantic *M. oculata* are also found in all other regions (one haplotype) or are restricted to the Bay of Biscay and Rockall bank (two haplotypes), with one haplotype unique to the Mid Atlantic site. Private (unique) haplotypes were observed in all regions where *M. oculata* was sampled but not at all sites. Seven haplotypes were well represented, and there was no obvious sign of haplotype radiation (Fig. 2b). Similarly to *L. pertusa*, the majority of ITS sequence variation for *M. oculata* occurred in Atlantic sites. The Bay of Biscay and Rockall bank presented the highest number of haplotypes (15 and 11, respectively) and the only region-specific haplotype (Appendix table S7). Nonetheless, the highest haplotype diversity (H=0.9) was observed in *M. oculata* from the Mid Atlantic.

Along the NE Atlantic *L. pertusa*, populations were little differentiated while within the Bay of Biscay genetic structure was weak for *M. oculata* (nearly all pairwise F_{ST} not significantly different from zero; Appendix Tables S2-S3). *Madrepora oculata* showed a regional pattern of population genetic structure concordant with microsatellite analyses (high F_{ST} between populations from distinct regions). Overall, 5% of *L. pertusa* and nearly 40% of *M. oculata* genetic variation occurred among regions (AMOVA; Appendix Table S5). .

Haplotypic and molecular diversities varied among locations (Tables 3 and 4). For *L. pertusa*, haplotypic diversity was high (up to 0.6 in the NE Atlantic and up to 0.7 in the Mediterranean Sea) due to haplotype radiations. Haplotypic diversity was also high in *M. oculata* populations (0.3-0.7 in High Latitudes, 0.9 in the Mid Atlantic site, where there were four haplotypes for five individuals). A comparable pattern of variation of molecular diversity was observed for both species. In the NE Atlantic, nucleotide diversity was lower than in the Mediterranean Sea sites for *L. pertusa*. For *M. oculata,* nucleotide diversity was higher in the west Mediterranean and Mid Atlantic populations.

Demographic inferences

The tests of conformity to selective neutrality suggest different demographic histories for *L. pertusa* and *M. oculata*. The Mediterranean populations of *L. pertusa* did not produce significant departures from mutation-drift equilibrium (Fu, 1996), while most populations in the Bay of Biscay showed negative Fs values significantly departing from mutation-drift equilibrium. This is consistent with the network and indicates a demographic expansion of Atlantic populations. Only two *M. oculata* sites showed Tajima D values significantly departing from constant effective population size that would indicate a demographic expansion: one in the east Mediterranean and one in the Bay of Biscay (Crozon canyon; Tables 3 and 4).

Model-based inference pointed to an ancient (up to 30 ka; Appendix Table S2) divergence of *L. pertusa* east and west Mediterranean Sea populations, in agreement with DAPC. The west Mediterranean population was identified as the source from which all other NE Atlantic populations emerged, either directly (Bay of Biscay and High latitudes; approx. 21 ka) or through admixture (Rockall bank; much later at 9 ka), agreeing with the Bayesian clustering, where the west Mediterranean ancestry (blue) is found throughout the Atlantic sites, and with ITS network, where most Mediterranean haplotypes are shared with Bay of Biscay corals. The shared Rockall genetic ancestry (grey) between Biscay and the High latitudes populations identified with Bayesian clustering agrees with the admixed origin for Rockall *L. pertusa* found with ABC. Population size estimates were much smaller for Mediterranean populations (N=2,500 to 7,000) than NE Atlantic ones (N=70,000-85,000). The Bay of Biscay demographic expansion scenario with admixture was supported with high

probability relative to around 0.2 support for scenarios including stepping-stone colonisation and changes in population sizes (Appendix Figs. S3-S4). Confidence in scenario choice was high, with low error rates (posterior predictive error = 0.29). Post-LGM range colonisation followed a long-range model of northern range colonisation, whereby Bay of Biscay and High latitudes were colonised directly from the west Mediterranean Sea populations, while at a later stage the Rockall bank was colonised from admixture between Bay of Biscay, High latitudes and west Mediterranean populations (Fig. 1 bottom inset).

Analyses with ABC pointed to the Mediterranean Sea *M. oculata* populations being the main source population (N=8,600) from which all other NE Atlantic populations emerged. The Mediterranean source population scenario, with colonisation of the Atlantic margins via Bay of Biscay agrees with Bayesian clustering, where the Mediterranean genetic ancestry (red) is found in moderate proportions in Bay of Biscay populations and is absent from the Mid Atlantic and Rockall populations. The scenario of a Mediterranean source population with colonisation of the NE Atlantic and admixture was supported with high probability (0.9) relative to low support for scenarios including changes in population sizes or competing admixture scenarios (Appendix Figs. S3-S4). Confidence in scenario choice was high, with low error rates (0.3). Post-LGM range colonisation along the European margins followed a stepping-stone model of northern range colonisation, whereby Bay of Biscay was colonised directly from Mediterranean Sea populations (22 ka), while the Bay of Biscay *M. oculata* later colonised the Rockall bank (7 ka). The Rockall bank populations then originated other NE Atlantic *M oculata* populations. That happened either through admixture with the Bay of Biscay (Mid Atlantic) only about 2 ka, or directly (High latitudes) much more recently (0.3 ka; Fig. 1 top inset). The genetic footprint of those events are seen on the main haplotype shared between High latitudes and Rockall but absent from Bay of Biscay corals, by a haplotype restricted to the Bay of Biscay, Rockall bank and Mid Atlantic (haplotype V in Appendix Figure S6), and by the position of Mid Atlantic samples in the DAPC between Rockall and Biscay samples.

Discussion

In terms of molecular analyses, Cold-Water corals (CWC) in NE Europe have been understudied. In this study we extend the available information from this area considerably, and present the first inferences and empirical analyses of deep-sea coral phylogeography in the area. While the Bay of Biscay genetic component presented here has been previously described in extant populations from the region (Morrison et al., 2011; Becheler et al., 2017), we gain further insights into its temporal depth. Given their recurrent association and similarities (Arnaud-Haond *et al.*, 2017), the two main CWC reef building species in the North Atlantic, *Lophelia pertusa* and *Madrepora oculata,* have been hypothesised to share similar phylogeographic histories (De Mol *et al.*, 2002; Henry *et al.*, 2014). Yet, our results depart from that expectation. Far-reaching gene flow along the European margin results in a poor genetic differentiation in distant NE Atlantic *L. pertusa* populations (Bay of Biscay and High latitudes), while high differentiation characterizes populations of *M. oculata*. We hypothesize that both species were affected by glacial events differently, and/or that the geographic location of the source and date of post-glacial expansion of NE Atlantic reefs differed. Verifying such hypotheses is important if we are to forecast the responses of CWC facing on-going climate changes.

Despite the deep-sea being considered as relatively environmentally stable over time, there is evidence that CWC undergo demographic changes similarly to those experienced by their coastal water counterparts (Wilson & Eigenmann Veraguth, 2010; Sabelli & Taviani, 2014; Vertino *et al.*, 2014; Quattrini *et al.*, 2015). Here we focused on the LGM, and explored two scenarios that could explain the observed patterns of genetic diversity and structure for *L. pertusa* and *M. oculata*, respectively:

i) Before the LGM (and to about 50 ka, which is the oldest period accounted for by existing data), NE Atlantic populations were absent from the current northern range of their modern distribution and present-day patterns of genetic variation were caused by expansion northwards, originated most likely from the west Mediterranean Sea and/or adjacent NW coast of Africa, and a later Mediterranean-NE Atlantic admixture;

ii) Before the LGM, NE Atlantic populations were absent from the current northern range of their modern distribution and present-day patterns of genetic variation were caused by "stepping-stone" northwards colonisation with modest demographic expansions and by a much later admixture between NE Atlantic populations with possible contribution from other unsampled populations.

Scenario i)

Geological studies report the absence of deep CWC reef growth in the NE Atlantic during glaciations of the Late Pleistocene (approx. 126 - 12 ka; with the Last Glacial Maximum approx. 26.5-19 ka; Clark et al., 2009; Frank *et al.*, 2009). Contrastingly, between 50-12 ka, *L. pertusa* reefs flourished in the Mediterranean Sea (Appendix Supplementary Paleo-History). The Mediterranean Outflow Water (MOW 800-1300 m depth; Price et al., 1993) volumes were smaller than at present (Rogerson *et al.*, 2004) but concentrated in channels with high local flow (Zahn *et al.*, 1997). In the Gulf of Cadiz and on the Moroccan shelf, reef growth was estimated to have started around 40-50 ka (Fig. 1) when glacial conditions there were particularly favourable for coral growth, unlike in the NE Atlantic (Schröder-Ritzrau *et al.*, 2005; Eisele *et al.*, 2011; Ramos *et al.*, 2017; Weinberg *et al.*, 2018). The rapid increase in post-glacial Atlantic Meridional Overturning Circulation resulted in increased transport of suspended particles and is speculated to have boosted the expansion of *L. pertusa* from these southern locations (Mediterranean Sea and/or adjacent NW coast of Africa) into the NE Atlantic (Eisele *et al.*, 2011; Fink *et al.*, 2013; Henry *et al.*, 2014).

Continuous and vertical growth of CWC reefs occurred in the Bay of Biscay area during at least the past 7,000 years, shown by geological analyses of the core. Genetic evidence of recent *L. pertusa* demographic expansions in the Bay of Biscay, at the end of the LGM (approx. 21 ka), is substantiated by Internal Transcribed Spacer sequences with haplotype network and conformity tests, attributed to a founder event, i.e. a dominant haplotype found in all regions (from the Mediterranean Sea to the High Latitudes). Such demographic expansion would have produced satellite haplotypes with low genetic distance, as observed in *L. pertusa*. The vast nearly-panmictic ensemble occurring along the NE Atlantic indicates a recent common history for Atlantic *L. pertusa* reefs. This is supported by studies of reproduction and larval development that indicate that *L. pertusa* larvae have high dispersal potential (Waller & Tyler, 2005; Larsson *et al.*, 2014; Strömberg & Larsson, 2017). Despite these experiments in aquaria with *L. pertusa* that have shown larvae swimming towards the surface, it remains unknown whether larvae are neutrally buoyant and if in their natural environment remain at spawning depth, concurrent with the depth of North Atlantic currents in figure 1. Larval dispersal trajectories may have evolved to track specific water masses (Dullo *et al.*, 2008), occurring at intermediate depths with potential settling sites. Such high larval dispersal ability favours large-scale expansion and shared genetic ancestry, such as that between Bay of Biscay and High latitudes *L. pertusa*.

The genetic distinctiveness of Rockall bank *L. pertusa* (seen on microsatellites and ITS loci) indicates a more complicated history. The rarity of the dominant haplotype in Rockall bank suggests either another source for colonisation, strong post-colonisation drift or local adaptation. Approximate Bayesian Computation favours an evolutionary scenario whereby the Rockall population is colonised via admixture of the Bay of Biscay group and west Mediterranean corals, around the time of the onset of the modern Atlantic Meridional Overturning Circulation (AMOC; Repschläger et al., 2017). The Mediterranean Water traveling northwards along the Iberian Peninsula and Bay of Biscay does not reach the Rockall bank (Frank et al., 2009). Instead, Rockall hydrodynamics are more influenced by northward moving Atlantic waters, including the rich North Atlantic Current (NAC). The NAC is part of the Gulf Stream, which may promote occasional genetic material from the West North Atlantic *L. pertusa* reefs (Morrison et al., 2011). Analyses encompassing the full distributional range of *L. pertusa* are essential to clarify missing links in population relatedness at trans-Atlantic scales.

The ancient divergence of Mediterranean *L. pertusa* populations from the eastern and western basins estimated by the ABC model to have taken place during the Last Glacial Maximum (around 24 ka) is

reasonable. In the temperate Eastern Atlantic, including the Mediterranean Sea, CWC growth sustained glacial-interglacial cycles (Frank et al., 2011). Such a steady allopatry may have been maintained by vicariance driven by ocean currents acting upon the earliest life stage of *L. pertusa* or by local adaptation. Finer-scale analyses are needed to identify and quantify the importance of such variables. All together, the data support a post-glacial recolonisation of the NE Atlantic by *L. pertusa*. Mediterranean *L. pertusa* are divergent from most NE Atlantic populations (ITS, microsatellites). Given that sampling is at best partial, it is difficult to speculate about the precise origin of NE Atlantic populations. The Mediterranean lineages and genotypes found in low proportion across the NE Atlantic reefs, the high haplotypic diversity mainly in the western basin of the Mediterranean Sea, concur with ABC analyses that the glacial refugia for NE Atlantic *L. pertusa* colonisation may have been located in the west Mediterranean Sea or in adjacent regions (e.g. the coral mounds in the Gulf of Cadiz and NW Africa; Eisele *et al.*, 2011). *Lophelia pertusa* populations in this region thrived during glacial periods and might have provided larvae dispersing in Mediterranean Water northwards towards the Bay of Biscay (Fig. 1).

Contrastingly, *M. oculata* populations are more strongly structured and there is no evidence of a large demographic expansion.

Scenario ii)

Concurrent to *L. pertusa*, Mediterranean Sea *M. oculata* populations were the main source from which all other NE Atlantic populations emerged around the end of the LGM, as estimated by model-based inference (Fig. 1 top inset). Mediterranean *M. oculata* thus represent the putative LGM refugium, which may have included other unsampled adjacent populations present during glacial periods (Gulf of Cadiz, NW Africa). As for *L. pertusa*, absence of samples from the NW coast of Africa meant that inference regarding the role of this potential refugium could not be made. The estimated time for NE Atlantic colonisation, approx. 21 ka, suggests that Mediterranean *M. oculata* represent a "stable rear-edge" population (Hampe & Petit 2005). Mediterranean harbours high levels of DNA diversity and the greatest number of unique haplotypes and private alleles, a testament to the long-term stability of Mediterranean populations (Hewitt 2000). But unlike *L. pertusa*, there is no substantial differentiation of east and west Mediterranean *M. oculata*, possibly linked to differences in reproductive or early life traits. Information on reproduction and early life history is much needed to reduce model uncertainty and allow a better understanding of CWC past and present connectivity.

Analyses identified that *M. oculata*'s northern range edge was colonised in a stepping-stone manner (Bay of Biscay, followed by Rockall and later the High latitudes) instead of long-range colonisation directly from glacial refugia as in *L. pertusa* northern populations. Unique haplotypes were almost evenly spread across the distribution range, indicating that *M. oculata* maintained other glacial (cryptic) refugia throughout its current range and underwent only localized, modest, postglacial expansions. The result is the co-existence of divergent genetic lineages across the NE Atlantic, one dominating the higher latitudes and another in the Bay of Biscay, both with lower frequency in other regions. Such pattern is consistent with distinct areas of persistence for *M. oculata*, locally or regionally, followed by a redistribution of divergent lineages after periods of allopatry (Petit *et al.*, 2003). The low occurrence of unique haplotypes and alleles found in *M. oculata* is a result of the more recent admixture and colonisation events (Mid Atlantic, High latitudes), estimated by ABC to have taken place during the late Holocene. The large-scale spatial genetic structure was shaped by the refugium-driven vicariance. Long-distance dispersal and gene flow that may disturb this pattern of population structure may be unlikely in *M. oculata*, if this CWC presents different reproduction and dispersal modes to those of *L. pertusa*, for instance, lower pelagic larval duration, brooding. A hypothetical poorer ability to disperse associated with the complex geomorphology (canyons, seamounts) along with extreme depth gradient present in habitats along the North East Atlantic (hundreds to thousands of meters), has probably caused fragmentation, reduced gene flow and further reinforced the large-scale pattern of NE Atlantic population structure in *M. oculata*. For instance, the Lampaul canyon has the highest composition of soft substrate and near absence coral framework compared to the other Bay of Biscay canyons studied here (van den Beld et al., 2017). Such

differences may have created (past) barriers to gene flow. However, separating the exact effects of geography and the environment on population structure is difficult. Finer-scale analyses are needed to estimate the contribution of such variables and putative allopatric refugia.

The formation of the admixed Mid Atlantic population was dated to c. 2 ka (0.7–11 ka); even accounting for wide confidence interval of the estimated time, it is well within the Holocene. During this period, the modern AMOC was established and can have contributed to colonisation of deep coral habitat along the Mid Atlantic Ridge and to admixture with older populations either from the European margins (Rockall bank, Bay of Biscay canyons) or from the NW Atlantic (which we did not sample here). The southward branch of the vigorous NAC may have favoured the link between European margins and Mid Atlantic. The absence of Mediterranean ancestry together with the substantial presence of High latitudes ancestry in Mid Atlantic and Rockall *M. oculata* substantiates a less important connection with Mediterranean populations via the weak flow of Mediterranean Water. The fact that the European margins genetic components and haplotypes are consistently shared among Mid Atlantic *M. oculata* makes it tempting to equate this genetic component with the colonisation or at least the spread of *M. oculata* in the Mid Atlantic. However, such a model may be overly simplistic. As shown in our analyses, the admixture patterns found in *M. oculata* are complex and more than a single admixture event is possible, with sources on both sides of the N Atlantic. The lower coral abundance and available habitat as compared to the NE Atlantic margins, may have further contributed to post-colonisation drift. More detailed analyses of Mid Atlantic CWC are needed to clarify the N Atlantic phylogeography of the deep-sea.

The colonisation of higher latitudes much more recently (*c.* 0.3 ka, 0.07-3 ka) from Rockall populations left genetic footprints; main *M. oculata* haplotype shared between High latitudes and Rockall but absent from Bay of Biscay. The timing difference of High latitudes colonisation among *L. pertusa* and *M. oculata* suggests that differences in environmental tolerance exist: *L. pertusa* reached the High latitudes at the end of the LGM (*c.* 21 ka; 9-29 ka). In fact, *L. pertusa* has thermal acclimation in respiration and calcification mechanisms that mechanisms are absent in *M. oculata* (Nauman et al., 2014). The Holocene colonisation of the higher latitudes of Europe (e.g., Norway; Fig. 1) is well documented (Schröder-Ritzrau *et al.*, 2005). Although reassuring for interpreting our findings, ABC model-based inferences rely on assumptions that cannot easily be controlled in natural populations. Our findings should be interpreted as probable hypotheses rather than clear proof of past demographic events. Further theoretical and experimental work are needed that can contribute to a better understanding of CWC phylogeography and connectivity (e.g., early life history traits). Analyses making use of high-density data will allow reconstructing the phylogeographic history of CWC with more precision. Moreover, our study highlights the need to explore the genetic nature of CWC found in the Western Mediterranean (Alboran Sea) and the Gulf of Cadiz to determine their contribution to larval connectivity and past re-colonisation of the NE Atlantic.

Conclusion The novel genetic data presented here from deep-sea corals from European margins opens new insights into Cold-Water coral population history. Our results show a northward post-LGM expansion of *Lophelia pertusa* and *M. oculata* from the west Mediterranean Sea into the NE Atlantic margin. While *L. pertusa* moderate to high gene flow homogenized nearly the whole Atlantic genetic pool, *M. oculata* progressed slower, particularly in High latitudes. *Lophelia pertusa* expanded swiftly along the NE Atlantic at a rate of 0.7 to 2 km per year (considering 4,000 km in the past 10 to 30 ka). The period of Atlantic-Mediterranean separation led to a strong genetic differentiation between extant coral populations in the respective regions. This differentiation can be explained either by a founder effect at the NE Atlantic, or an unsampled genetic source in the Mediterranean Sea or around NW Africa. The remarkable mosaic of distinct genotypes of *M. oculata* supports the existence of a more complex history, shaped by putative cryptic refugia, admixture and possible different dispersal ability. With current data limitations, it is not yet possible to determine the most important factor underlying the apparent lack of gene flow along the European margin for *M. oculata* populations. Further CWC from the North Atlantic are needed in order to conclude, to what extent these signals of migration and admixture are representative of N Atlantic CWC as a whole. Nonetheless, the contrasting patterns of genetic diversity observed here strongly support the existence of a different influence of past

environmental changes and differing present-day dispersal of *L. oculata* and *M. oculata*. Our study provides an important warning for managers that even taxa with seemingly similar ecological roles and tolerances may well differ in their response to global change. Therefore, multi-species models are required to ensure conservation measures such as truly representative and connected networks of Marine Protected Areas.

Author contributions:

Designed research RB, SAH,

Performed research RB, SAH, JB, A-L C, OM, MC

Contributed new reagents or analytic tools SAH, JFB, NF, MT, AS, AG, JB

Analysed data RB, JB, SAH

Wrote the paper JB, RB, SAH

Data Accessibility Statement

Microsatellite data are accessible online at GenBank under accession numbers: KF944311, KF944317, KF944323, KF944330, KF944331 and KF944344.

viii. Tables and captions

Table 1 - Genetic diversity at microsatellite loci for *Lophelia pertusa*. n - sample size; Âr - allelic richness; Âr(5) - standardized allelic richness to the lowest sample size (N=5); Âp - private allelic richness; He and Ho - expected and observed heterozygosity respectively; Fis - departure from HWE. P-values below 0.05, 0.01 and 0.001 are respectively represented by *, ** and ***.

Region	Site	n	Âr	Âr(5)	Âp	He	Ho	Fis
Eastern Mediterranean Sea	Santa Maria di Leuca (SML)	12	8.1	6.0 ± 0.2	4	0.80 ± 0.06	0.71 ± 0.31	0.15***
Western Mediterranean Sea	Lacaze-Duthiers canyon (LCD)	7	4.9	4.9 ± 0.00	2	0.72 ± 0.13	0.84 ± 0.19	-0.10
Bay of Biscay	Croisic canyon (CRS)	30	18.9	8.8 ± 0.12	5	0.89 ± 0.07	0.80 ± 0.14	0.12***
Bay of Biscay	Guilvinec canyon (GUI)	34	18.3	8.7 ± 0.12	4	0.89 ± 0.08	0.86 ± 0.04	0.05**
Bay of Biscay	Lampaul canyon (LMP)	7	8.8	8.8 ± 0.00	2	0.83 ± 0.09	0.80 ± 0.19	0.11**
Bay of Biscay	Crozon canyon (CRZ)	12	11.0	8.0 ± 0.13	2	0.84 ± 0.09	0.74 ± 0.14	0.16***
Bay of Biscay	Morgat-Douarnez canyon (MRG)	20	16.4	8.6 ± 0.16	4	0.87 ± 0.09	0.83 ± 0.20	0.07**
Bay of Biscay	Petite Sole 1 canyon (PS1)	26	17.4	8.7 ± 0.12	5	0.88 ± 0.09	0.83 ± 0.11	0.07***
Bay of Biscay	Petite Sole 2 canyon (PS2)	27	17.5	8.9 ± 0.10	4	0.90 ± 0.06	0.85 ± 0.09	0.07***
Rockall bank	Logachev Mounds (LOG)	22	14.8	8.1 ± 0.12	2	0.87 ± 0.07	0.77 ± 0.13	0.14***
High latitudes	Londsjup 1 (LON1)	7	8.5	8.5 ± 0.00	1	0.82 ± 0.09	0.77 ± 0.15	0.14**
High latitudes	Londsjup 2 (LON2)	20	14.5	8.2 ± 0.12	4	0.86 ± 0.10	0.74 ± 0.16	0.17***
High latitudes	Hafadsjup (HAF)	16	13.6	8.5 ± 0.12	1	0.89 ± 0.05	0.70 ± 0.22	0.25***

Table 2 - Genetic diversity at microsatellite loci for *Madrepora oculata*. n - sample size; Âr - allelic richness; Âr(5) - standardized allelic richness to the lowest sample size (N=5); Âp - private allelic richness; He and Ho - expected and observed heterozygosity respectively; Fis - departure from HWE. P-values below 0.05, 0.01 and 0.001 are respectively represented by *, ** and ***.

Region	Site	n	Âr	Âr(5)	Âp	He	Ho	Fis
Eastern Mediterranean Sea	Montenegro (MNG)	5	2.3	2.3 ± 0.0	2	0.31 ± 0.34	0.27 ± 0.39	0.26
Western Mediterranean Sea	Lacaze-Duthiers canyon (LCD)	6	3.5	3.3 ± 0.04	4	0.45 ± 0.32	0.56 ± 0.40	-0.16
Mid Atlantic Ocean	Azores (AZO)	5	2.7	2.7 ± 0.0	0	0.38 ± 0.27	0.47 ± 0.39	-0.12
Bay of Biscay	Croisic canyon (CRS)	39	6.3	3.7 ± 0.06	1	0.66 ± 0.10	0.67 ± 0.13	0.00
Bay of Biscay	Guilvinec canyon (GUI)	42	5.5	3.7 ± 0.06	0	0.67 ± 0.15	0.60 ± 0.28	0.12***
Bay of Biscay	Lampaul canyon (LMP)	11	3.8	3.2 ± 0.03	1	0.56 ± 0.28	0.58 ± 0.31	0.02
Bay of Biscay	Morgat-Douarnez canyon (MRG)	29	4.8	3.5 ± 0.05	0	0.61 ± 0.16	0.56 ± 0.23	0.10*
Bay of Biscay	Crozon canyon (CRZ)	23	5.5	3.5 ± 0.06	1	0.59 ± 0.24	0.52 ± 0.27	0.14**

Bay of Biscay	Petite Sole 1 canyon (PS1)	23	5.2	3.6 ± 0.05	0	0.63 ± 0.16	0.65 ± 0.21	-0.01
Bay of Biscay	Petite Sole 2 canyon (PS2)	32	6.2	3.7 ± 0.08	0	0.65 ± 0.14	0.59 ± 0.19	0.10*
Rockall bank	Logachev Mounds (LOG)	24	6.0	3.5 ± 0.07	0	0.54 ± 0.30	0.49 ± 0.31	0.11*
High latitudes	Londsjup 1 (LON1)	6	3.7	3.3 ± 0.04	0	0.45 ± 0.30	0.39 ± 0.29	0.22*
High latitudes	Londsjup 2 (LON2)	33	4.5	2.5 ± 0.06	2	0.38 ± 0.28	0.31 ± 0.30	0.18**
High latitudes	Hafadsjup (HAF)	17	4.5	3.1 ± 0.06	0	0.46 ± 0.32	0.44 ± 0.34	0.06

Table 3 - Genetic diversity and neutrality tests for ITS at each location of *Lophelia pertusa*. Asterisk (*) - P-values under 0.05. NA - Not applicable (Lampaul canyon had no polymorphic sites).

		No. Samples (n)	No. Haplotypes	No. Private haplotypes	Haplotype diversity (H)	Nucleotide diversity (π)	Tajima's D	FS
East Mediterranean Sea								
	Santa Maria di Leuca (SML)	15	4	0	0.4476	0.0011	-0.33	1.52
West Mediterranean Sea								
	Lacaze-Duthiers canyon (LCD)	7	6	2	0.7143	0.0028	-0.86	0.75
Bay of Biscay								
	Croisic canyon (CRS)	21	6	2	0.2714	0.0003	-1.73*	-2.82*
	Guilvinec canyon (GUI)	23	7	1	0.249	0.0004	-1.88*	-1.75*
	Morgat-Douarnez canyon (MRG)	30	10	4	0.2529	0.0003	-2.01*	-3.70*
	Crozon canyon (CRZ)	11	6	2	0.6182	0.0014	-1.85*	-0.92
	Lampaul canyon (LMP)	7	1	0	0	NA	NA	NA
	Petite Sole1 (PS1)	28	3	1	0.0909	0.0001	-1.16	-0.96
	Petite Sole2 (PS2)	22	5	2	0.2063	0.0004	-1.89*	-1.62*
Rockall bank								
	Logachev mounds (LOG)	21	5	3	0.4143	0.0006	-1.22	-1.01
High latitudes								
	Londsjup1 (LON1)	8	4	2	0.4643	0.0007	-1.45	-0.30
	Londsjup2 (LON2)	20	7	2	0.5105	0.0008	-1.41	-1.48

	HafadJup (HAF)	16	5	1	0.4417	0.0008	-1.22	-0.37
	Mean	14.5	5.5	1.7	0.4	0.0008	-0.78	-1.50
	s.d.	8.95	1.90	1.11	0.20	0.00073	0.991	1.594

Table 4 - Genetic diversity and neutrality tests for ITS at each location of *Madrepora oculata*. Asterisk (*) - P-values under 0.05. NA - Not applicable (Londsjup 2 had no polymorphic sites).

	No. Samples (n)	No. Haplotypes	No. Private haplotypes	Haplotype diversity (H)	Nucleotide diversity (π)	Tajima's D	FS
East Mediterranean Sea	5	5	4				
Montenegro (MNG)	5	5	4	0.71	0.0018	-1.55*	-0.13
West Mediterranean Sea	4	4	4				
Lacaze-Duthiers canyon (LCD)	4	4	4	0.83	0.0025	0.37	0.65
Mid Atlantic Ocean	5	4	2				
Azores (AZO)	5	4	2	0.90	0.0020	-0.56	-0.85
Bay of Biscay	91	33	8				
Croisic canyon (CRS)	10	10	0	0.60	0.0011	0.47	0.84
Guilvinec canyon (GUI)	20	16	2	0.68	0.0016	0.25	-0.43
Morgat-Douarnez canyon (MRG)	10	13	0	0.56	0.0013	0.30	0.17
Crozon canyon (CRZ)	12	8	0	0.14	0.0004	-1.67*	0.90
Lampaul canyon (LMP)	10	10	2	0.47	0.0010	-0.64	0.83
Petite Sole1 (PS1)	7	8	2	0.64	0.0014	0.23	1.23
Petite Sole2 (PS2)	12	12	2	0.42	0.0010	-1.73	-0.16
Rockall bank	27	21	2				
Logachev mounds (LOG)	27	21	2	0.66	0.0014	-0.46	-0.51
High latitudes	63	12	4				
Londsjup1 (LON1)	8	8	2	0.68	0.0018	-0.49	1.65
Londsjup2 (LON2)	34	4	0	NA	NA	N.A.	N.A.
HafadJup (HAF)	21	8	2	0.27	0.0006	-1.02	0.53
Mean	14.1	11.4	2.4	0.58	0.0014	-0.46	0.34
s.d.	8.90	6.82	1.90	0.212	0.00057	0.784	0.722

ix. Figures and captions

Figure 1 - Contemporary distribution of *M. oculata* (black diamonds) and *L. pertusa* (grey circles) in the NE Atlantic, (2017 UNEP database; http://data.unep-wcmc.org) and the path of the main North East Atlantic Ocean currents (adapted from Montero-Serrano *et al.*, 2011, Somoza *et al.*, 2014 and Cossa et al., 2018): MOW - Mediterranean Outflow Water; MW - Mediterranean Sea Water; NAC - North Atlantic Water; MNAW - Modified North Atlantic Water; EAAIW - Eastern Antarctic Intermediate Water; LSW - Labrador Sea Water; ISOW - Iceland-Scotland Overflow Water. Site abbreviations as in Table 1. Dates correspond to estimated ages for coral mound growth (adapted from Schröder-Ritzrau *et al.*, 2005). Insets are the selected demographic history models for each cold-water coral species. ka - thousand years ago. Map created on QGIS with Mollweide's equal area projection.

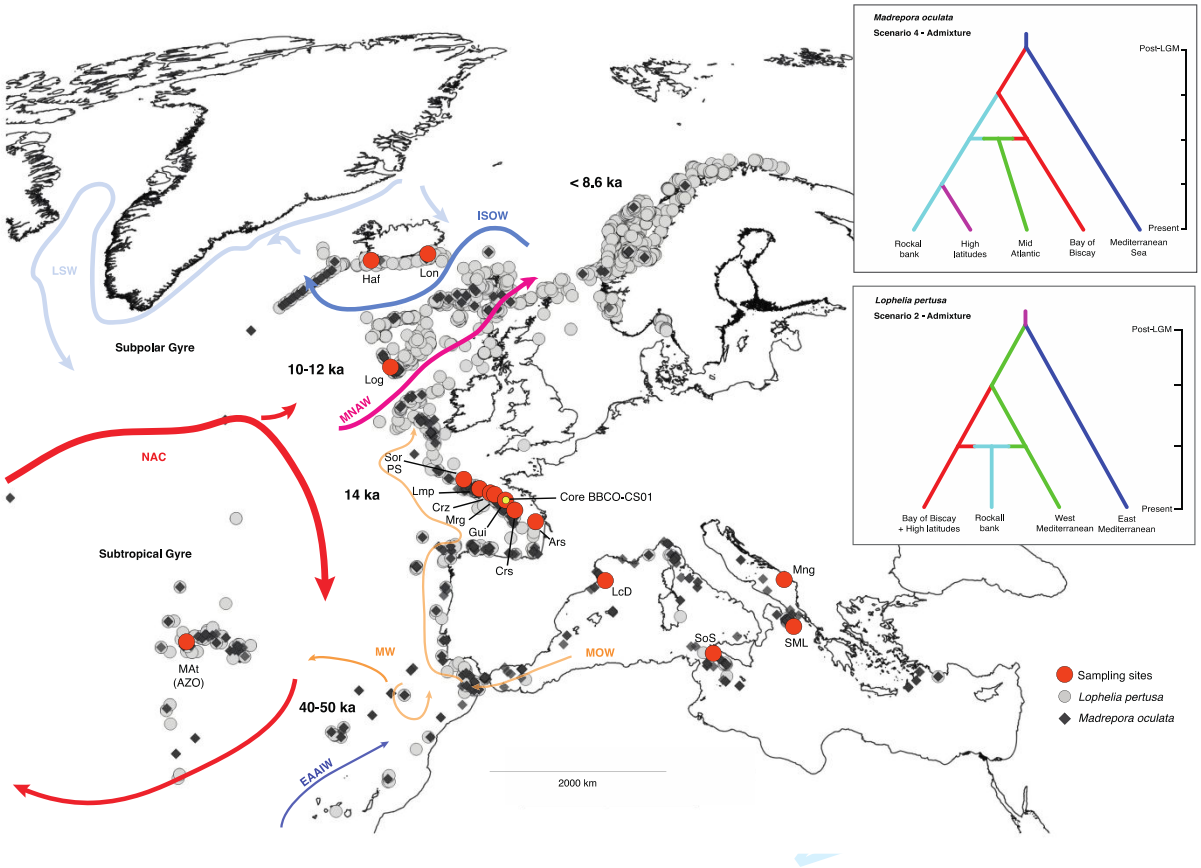

Figure 2 - Genetic subdivision among regional samples. (a) Microsatellites population membership diagrams from TESS displaying the probability of each individual into K = 4 clusters for *Madrepora oculata* (left) and *Lophelia pertusa* (right) (denoted by different colours). Each individual

is depicted by a horizontal line partitioned into K coloured sections, with the length of each section proportional to the estimated ancestry proportion to each cluster. Sample names refer to sites indicated in table and Fig. 1. Samples from the Bay of Biscay canyons (left diagram) are geographically ordered from north to south according to what is shown on Fig. 1. Black horizontal lines separate adjacent sites (MAt - Mid Atlantic, Med. - Mediterranean). (b) Parsimony haplotype networks of Internal Transcribed Spacer ribosomal sequences for *M. oculata* (left) and *L. pertusa* (right). The size of the circle is proportional to the observed number of sequences for the corresponding haplotype. Pie charts illustrate the proportion of a haplotype found in each region. The length of links is proportional to the number of mutations separating two haplotypes; the shortest represent a single mutation. Mediterranean includes eastern and western basin samples.

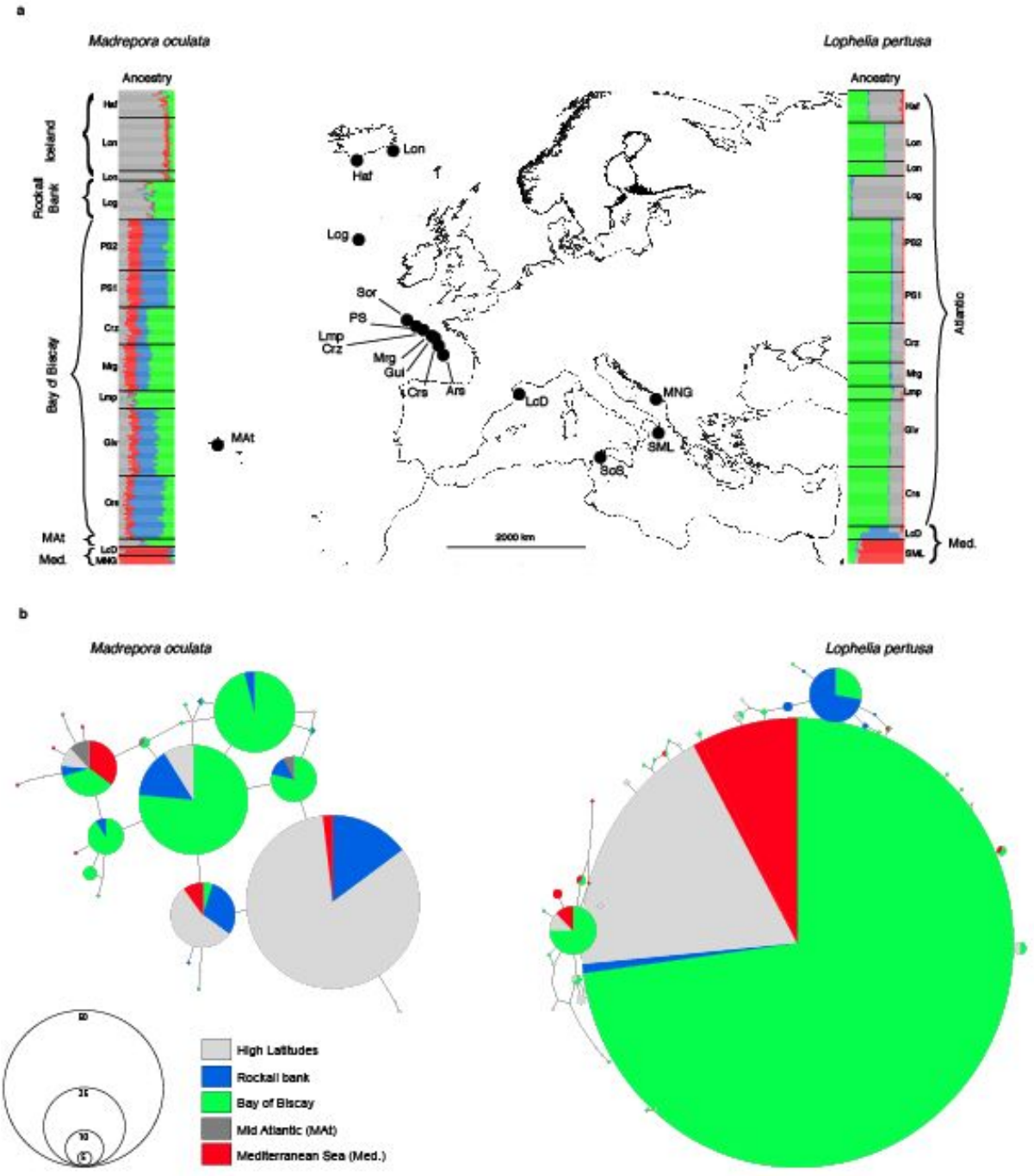

Figure 3 - Genetic subdivision among regional samples. Top - Discriminant Analyses of Principal Components (DAPC). A minimum-spanning tree based on the squared distances between groups connects group centres (crosses). Insets show the variance explained by the principal components included in the analyses (black). Because the identified optimal number of genetic clusters (K) for *Lophelia pertusa* is K=2 (see additional inset with sample density along the first discriminant function), the DAPC plot for *L. pertusa* shows samples color-coded by sampling site. Bottom - Population membership diagrams displaying the probability of each individual colour-coded by sampling site.

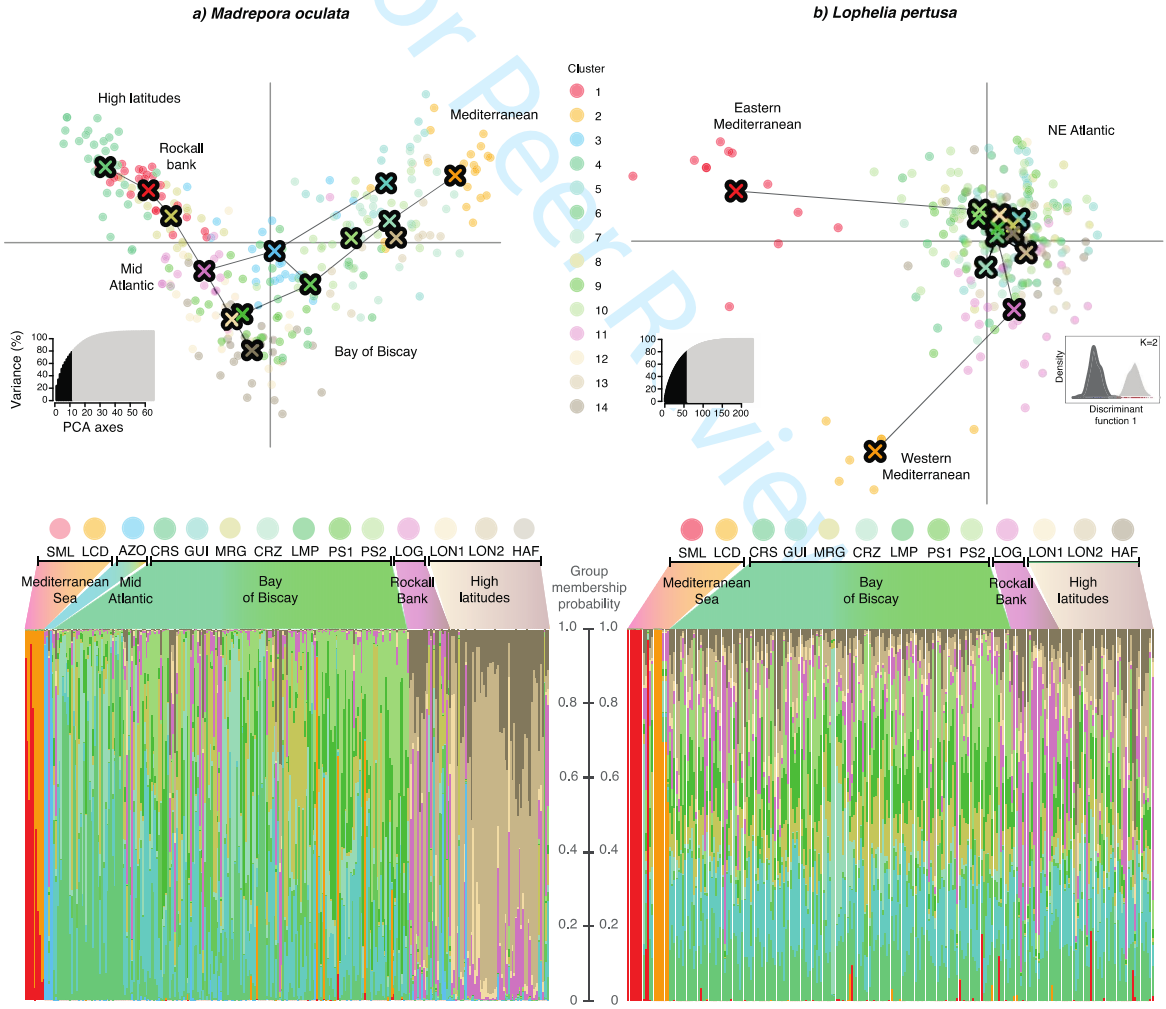

x. References

Arnaud-Haond, S., Van den Beld, I.M.J., Becheler, R., Orejas, C., Menot, L., Frank, N., Grehan, A. & Bourillet, J.F. (2017) Two "pillars" of cold-water coral reefs along Atlantic European margins: Prevalent association of Madrepora oculata with Lophelia pertusa, from reef to colony scale. *Deep-Sea Research Part II: Topical Studies in Oceanography*, **145**, 110–119.

Becheler, R., Cassone, A.L., Noël, P., Mouchel, O., Morrison, C.L. & Arnaud-Haond, S. (2017) Low incidence of clonality in cold water corals revealed through the novel use of a standardized protocol adapted to deep sea sampling. *Deep-Sea Research Part II: Topical Studies in Oceanography*, **145**, 120–130.

van den Beld, I.M.J., Bourillet, J.-F., Arnaud-Haond, S., de Chambure, L., Davies, J.S., Guillaumont, B., Olu, K., & Menot, L. (2017) Cold-Water Coral Habitats in Submarine Canyons of the Bay of Biscay. *Frontiers in Marine Science*, **4**.

Belkhir K., Borsa P., Chikhi L., Raufaste N., B.F. (2004) Genetix 4.05, logiciel sous Windows TM pour la génétique des populations.

Bouchet, P. & Taviani, M. (1992) The Mediterranean deep-sea fauna: pseudopopulations of Atlantic species? *Deep Sea Research Part A, Oceanographic Research Papers*, **39**, 169–184.

Chen, C., Durand, E., Forbes, F. & François, O. (2007) Bayesian clustering algorithms ascertaining spatial population structure: a new computer program and a comparison study. *Molecular Ecology Notes*, **7**, 747–756.

Clement, M., Posada, D., & Crandall, K.A. (2000) TCS: A computer program to estimate gene genealogies. *Molecular Ecology*, **9**, 1657–1659.

Clark, P.U. (2009) The Last Glacial Maximum. *Science*, **325**, 710–714.

Cordes, E.E., Jones, D.O., Schlacher, T., Amon, D.J., Bernardino, A.F., Brooke, S., Carney, R., DeLeo, D.M., Dunlop, K.M., Escobar-Briones, E.G., Gates, A.R., Genio, L., Gobin, J., Henry, L.-A., Herrera, S., Hoyt, S., Joye, S., KArk, S., Mestre, N.C., Metaxas, A., Pfeifer, S., Sink, K., Sweetman, A.K. & Witte, U.F. (2016) Environmental impacts of the deep-water oil and gas industry: a review to guide management strategies. *Frontiers in Environmental Science*, **4**, 1–54.

Cornuet, J.M., Pudlo, P., Veyssier, J., Dehne-Garcia, A., Gautier, M., Leblois, R., Marin, J.M., & Estoup, A. (2014) DIYABC v2.0: A software to make approximate Bayesian computation inferences about population history using single nucleotide polymorphism, DNA sequence and microsatellite data. *Bioinformatics*, **30**, 1187–1189.

Cossa, D., Heimbürger, L.E., Pérez, F.F., García-Ibáñez, M.I., Sonke, J.E., Planquette, H., Lherminier, P., Boutorh, J., Cheize, M., Lukas Menzel Barraqueta, J., Shelley, R., & Sarthou, G. (2018) Mercury distribution and transport in the North Atlantic Ocean along the GEOTRACES-GA01 transect. *Biogeosciences*, **15**, 2309–2323.

Dahl, M.P., Pereyra, R.T., Lundälv, T. & André, C. (2012) Fine-scale spatial genetic structure and clonal distribution of the cold-water coral Lophelia pertusa. *Coral Reefs*, **31**, 1135–1148.

Diekmann, O.E., Bak, R.P.M., Stam, W.T. & Olsen, J.L. (2001) Molecular genetic evidence for probable reticulate speciation in the coral genus Madracis from a Caribbean fringing reef slope. *Marine Biology*, **139**, 221–233.

Doyle, J.J. & Doyle, J.L. (1988) Natural interspecific hybridization in eastern north-american Claytonia. *American Journal of Botany*, **75**, 1238–1246.

Drummond, A.J., Rambaut, A., Shapiro, B., & Pybus, O.G. (2005) Bayesian coalescent inference of past population dynamics from molecular sequences. Molecular Biology and Evolution, 22, 1185–1192.

Dullo, W.C., Flögel, S. & Rüggeberg, A. (2008) Cold-water coral growth in relation to the hydrography of the Celtic and Nordic European continental margin. *Marine Ecology Progress Series*, **371**, 165–176.

Eisele, M., Frank, N., Wienberg, C., Hebbeln, D., López Correa, M., Douville, E. & Freiwald, A. (2011) Productivity controlled cold-water coral growth periods during the last glacial off Mauritania. *Marine Geology*, **280**, 143–149.

Excoffier, L., Laval, G. & Schneider, S. (2005) Arlequin (version 3.0): An integrated software package for population genetics data analysis. *Evolutionary Bioinformatics Online*, **1**, 47–50.

Fenberg, P.B., Caselle, J.E., Claudet, J., Clemence, M., Gaines, S.D., Antonio García-Charton, J., Gonçalves,

E.J., Grorud-Colvert, K., Guidetti, P., Jenkins, S.R., Jones, P.J.S., Lester, S.E., McAllen, R., Moland, E., Planes, S. & Sorensen, T.K. (2012) The science of European marine reserves: Status, efficacy, and future needs. *Marine Policy*, **36**, 1012–1021.

Fink, H.G., Wienberg, C., De Pol-Holz, R., Wintersteller, P. & Hebbeln, D. (2013) Cold-water coral growth in the Alboran Sea related to high productivity during the Late Pleistocene and Holocene. *Marine Geology*, **339**, 71–82.

Flot, J.-F., Dahl, M. & André, C. (2013) Lophelia pertusa corals from the Ionian and Barents seas share identical nuclear ITS2 and near-identical mitochondrial genome sequences. *BMC research notes*, **6**, 144.

François, O., Ancelet, S. & Guillot, G. (2006) Bayesian clustering using hidden Markov random fields in spatial population genetics. *Genetics*, **174**, 805–16.

Frank, N., Ricard, E., Lutringer-Paquet, A., van der Land, C., Colin, C., Blamart, D., Foubert, A., Van Rooij, D., Henriet, J.P., de Haas, H. & van Weering, T. (2009) The Holocene occurrence of cold water corals in the NE Atlantic: Implications for coral carbonate mound evolution. *Marine Geology*, **266**, 129–142.

Frank, N., Freiwald, A., Correa, M.L., Wienberg, C., Eisele, M., Hebbeln, D., Van Rooij, D., Henriet, J.-P., Colin, C., van Weering, T., de Haas, H., Buhl-Mortensen, P., Roberts, J.M., De Mol, B., Douville, E., Blamart, D., & Hatte, C. (2011) Northeastern Atlantic cold-water coral reefs and climate. *Geology*, 39, 743–746.

Fu, Y.X. (1996) New statistical tests of neutrality for DNA samples from a population. *Genetics*, **143**, 557–570.

Henry, L.A., Frank, N., Hebbeln, D., Wienberg, C., Robinson, L., de Flierdt, T. van, Dahl, M., Douarin, M., Morrison, C.L., Correa, M.L., Rogers, A.D., Ruckelshausen, M. & Roberts, J.M. (2014) Global ocean conveyor lowers extinction risk in the deep sea. *Deep-Sea Research Part I: Oceanographic Research Papers*, **88**, 8–16.

Herrera, S., Shank, T.M. & Sanchez, J.A. (2012) Spatial and temporal patterns of genetic variation in the widespread antitropical deep-sea coral Paragorgia arborea. *Molecular Ecology*, **21**, 6053–6067.

Hewitt, G.M. (2004) Genetic consequences of climatic oscillations in the Quaternary. *Philosophical Transactions of the Royal Society B: Biological Sciences*, **359**, 183–195.

Hewitt, G.M. (1999) Post-glacial re-colonisation of European biota. *Biological Journal of the Linnean Society*, **68**, 87–112.

Hewitt, G.M. (1996) Some genetic consequences of ice ages, and their role, in divergence and speciation. *Biological Journal of the Linnean Society*, **58**, 247–276.

Jombart, T. (2008) Adegenet: A R package for the multivariate analysis of genetic markers. *Bioinformatics*, **24**, 1403–1405.

Jombart, T., Devillard, S., & Balloux, F. (2010) Discriminant analysis of principal components: a new method for the analysis of genetically structured populations. *BMC genetics*, **11**, 94.

Kearse, M., Moir, R., Wilson, A., Stones-Havas, S., Cheung, M., Sturrock, S., Buxton, S., Cooper, A., Markowitz, S., Duran, C., Thierer, T., Ashton, B., Meintjes, P. & Drummond, A. (2012) Geneious Basic: An integrated and extendable desktop software platform for the organization and analysis of sequence data. *Bioinformatics*, **28**, 1647–1649.

Kitahara, M. V., Cairns, S.D., Stolarski, J., Blair, D., & Miller, D.J. (2010) A comprehensive phylogenetic analysis of the scleractinia (Cnidaria, Anthozoa) based on mitochondrial CO1 sequence data. *PLoS ONE*, 5, e11490.

Kousteni, V., Kasapidis, P., Kotoulas, G. & Megalofonou, P. (2015) Strong population genetic structure and contrasting demographic histories for the small-spotted catshark (*Scyliorhinus canicula*) in the Mediterranean Sea. *Heredity*, **114**, 333–343.

Larsson, A.I., Jarnegren, J., Strömberg, S.M., Dahl, M.P., Lundalv, T. & Brooke, S. (2014) Embryogenesis and larval biology of the cold-water coral Lophelia pertusa. *PLoS ONE*, **9**.

Lartaud, F., Meistertzheim, A.L., Peru, E. & Le Bris, N. (2017) In situ growth experiments of reef-building cold-water corals: the good, the bad and the ugly. *Deep Sea Research Part I: Oceanographic Research Papers*, **121**, 70–78.

Lartaud, F., Pareige, S., de Rafelis, M., Feuillassier, L., Bideau, M., Peru, E., De la Vega, E., Nedoncelle, K., Romans, P. & Le Bris, N. (2014) Temporal changes in the growth of two Mediterranean cold-water coral species, in situ and in aquaria. *Deep-Sea Research Part II: Topical Studies in Oceanography*, **99**, 64–70.

LeGoff-Vitry, M.C., Pybus, O.G. & Rogers, A.D. (2004) Genetic structure of the deep-sea coral Lophelia pertusa in the northeast Atlantic revealed by microsatellites and internal transcribed space sequences. *Molecular Ecology*, **13**, 537–549.

Maggs, C.A., Castilho, R., Foltz, D., Henzler, C., Jolly, M.T., Kelly, J., Olsen, J., Perez, K.E., Stam, W., Väinölä, R., Viard, F. & Wares, J. (2008) Evaluating signatures of glacial refugia for north atlantic benthic marine taxa. *Ecology*, **89**.

Meistertzheim, A.L., Lartaud, F., Arnaud-Haond, S., Kalenitchenko, D., Bessalam, M., Le Bris, N. & Galand, P.E. (2016) Patterns of bacteria-host associations suggest different ecological strategies between two reef building cold-water coral species. *Deep-Sea Research Part I: Oceanographic Research Papers*, **114**, 12–22.

Milligan, R.J., Spence, G., Roberts, J.M. & Bailey, D.M. (2016) Fish communities associated with cold-water corals vary with depth and substratum type. *Deep-Sea Research Part I: Oceanographic Research Papers*, **114**, 43–54.

De Mol, B., Van Rensbergen, P., Pillen, S., Van Herreweghe, K., Van Rooij, D., McDonnell, A., Huvenne, V., Ivanov, M., Swennen, R. & Henriet, J.P. (2002) Large deep-water coral banks in the Porcupine Basin, southwest of Ireland. *Marine Geology*, **188**, 193–231.

Montero-Serrano, J.C., Frank, N., Colin, C., Wienberg, C., & Eisele, M. (2011) The climate influence on the mid-depth Northeast Atlantic gyres viewed by cold-water corals. *Geophysical Research Letters*, **38**, L19604.

Morrison, C.L., Eackles, M.S., Johnson, R.L. & King, T.L. (2008) Characterization of 13 microsatellite loci for the deep-sea coral, Lophelia pertusa (Linnaeus 1758), from the western North Atlantic Ocean and Gulf of Mexico. *Molecular Ecology Resources*, **8**, 1037–1039.

Morrison, C.L., Ross, S.W., Nizinski, M.S., Brooke, S., Järnegren, J., Waller, R.G., Johnson, R.L. & King, T.L. (2011) Genetic discontinuity among regional populations of Lophelia pertusa in the North Atlantic Ocean. *Conservation Genetics*, **12**, 713–729.

Morton, B. & Britton, J.C. (2000) Origins of the Azorean Intertidal Biota: the Significance of Introduced Species, Survivors of Chance Events. *Arquipélago. Life and Marine Science*, **2**, 29–51.

Naumann, M.S., Orejas, C., & Ferrier-Pagés, C. (2014) Species-specific physiological response by the cold-water corals Lophelia pertusa and Madrepora oculata to variations within their natural temperature range. *Deep-Sea Research Part II: Topical Studies in Oceanography*, **99**, 36–41.

Nei, M. (1978) Estimation of average heterozygosity and genetic distance from a small number of individuals. *Genetics*, **89**, 583–590.

Nei, M. (1987) *Molecular Evolutionary Genetics*, Columbia University Press, New York, NY.

Petit, R.J., Aguinagalde, I., Beaulieu, J.-L. De, Bittkau, C., Brewer, S., Cheddadi, R., Ennos, R., Fineschi, S., Grivet, D., Lascoux, M., Mohanty, A., Muller-Starck, G., Demesure-Musch, B., Palmé, A., Martín, J.P., Rendell, S. & Vendramin, G.G. (2003) Glacial refugia: Hotspots but not melting pots of genetic diversity. *Science*, **300**, 1563–1565.

Price, J.F., Baringer, M.O., Lueck, R.G., Johnson, G.C., Ambar, I., Parrilla, G., Cantos, A., Kennelly, M.A., & Sanford, T.B. (1993) Mediterranean Outflow Mixing and Dynamics. *Science (New York, N.Y.)*, **259**, 1277–1282.

Pritchard, J.K., Stephens, M. & Donnelly, P. (2000) Inference of population structure using multilocus genotype data. *Genetics*, **155**, 945–59.

Pusceddu, A., Bianchelli, S., Martín, J., Puig, P., Palanques, A., Masqué, P. & Danovaro, R. (2014) Chronic and intensive bottom trawling impairs deep-sea biodiversity and ecosystem functioning. *Proceedings of the National Academy of Sciences of the United States of America*, **111**, 8861–6.

Quattrini, A.M., Baums, I.B., Shank, T.M., Morrison, C.L. & Cordes, E.E. (2015) Testing the depth-differentiation hypothesis in a deepwater octocoral. *Proceedings of the Royal Society B*, **282**, 20150008.

Ramos, A., Sanz, J.L., Ramil, F., Agudo, L.M. & Presas-Navarro, C. (2017) *Deep-Sea Ecosystems Off*

Mauritania. *Deep-Sea Ecosystems Off Mauritania* (ed. by A. Ramos), J.L. Sanz), and F. Ramil), pp. 481–525. Springer Netherlands.

Repschläger, J., Garbe-Schönberg, D., Weinelt, M., & Schneider, R. (2017) Holocene evolution of the North Atlantic subsurface transport. *Climate of the Past*, **13**, 333–344.

Rogerson, M., Rohling, E.J., Weaver, P.P.E. & Murray, J.W. (2004) The Azores Front since the Last Glacial Maximum. *Earth and Planetary Science Letters*, **222**, 779–789.

Sabelli, B. & Taviani, M. (2014) *The making of the Mediterranean Molluscan Biodiversity*. *The Mediterranean Sea: Its History and Present Challenges* (ed. by S. Goffredo) and Z. Dubinsky), pp. 1–678.

Santos, A., Cabezas, M.P., Tavares, A.I., Xavier, R., & Branco, M. (2015) TcsBU: A tool to extend TCS network layout and visualization. *Bioinformatics*, **32**, 627–628.

Schröder-Ritzrau, A., Freiwald, A. & Mangini, A. (2005) *U/Th-dating of deep-water corals from the eastern North Atlantic and the western Mediterranean Sea*. *Cold-Water Corals and Ecosystems* (ed. by A. Freiwald) and J.M. Roberts), pp. 157–172. Springer-Verlag Berlin Heidelberg.

Shum, P., Pampoulie, C., Kristj, A. & Mariani, S. (2015) Three-dimensional post-glacial expansion and diversification of an exploited oceanic fish. *Molecular Ecology*, **24**, 3652–3667.

Strömberg, S.M. & Larsson, A.I. (2017) Larval Behavior and Longevity in the Cold-Water Coral Lophelia pertusa Indicate Potential for Long Distance Dispersal. *Frontiers in Marine Science*, **4**, 32–33.

Stumpf, R., Frank, M., Schönfeld, J. & Haley, B.A. (2010) Late Quaternary variability of Mediterranean Outflow Water from radiogenic Nd and Pb isotopes. *Quaternary Science Reviews*, **29**, 2462–2472.

Tajima, F. (1983) Evolutionary relationship of DNA sequences in finite populations. *Genetics*, **105**, 437–460.

Vertino, A., Stolarski, J., Bosellini, F.R. & Taviani, M. (2014) Mediterranean Corals Through Time: From Miocene to Present. *The Mediterranean Sea: Its History and Present Challenges*, 1–678.

Voelker, A.H.L., Lebreiro, S.M., Schönfeld, J., Cacho, I., Erlenkeuser, H. & Abrantes, F. (2006) Mediterranean outflow strengthening during northern hemisphere coolings: A salt source for the glacial Atlantic? *Earth and Planetary Science Letters*, **245**, 39–55.

Waller, R.G. & Tyler, P.A. (2005) The reproductive biology of two deep-water, reef-building scleractinians from the NE Atlantic Ocean. *Coral Reefs*, **24**, 514–522.

Wedding, L.M., Reiter, S.M., Smith, C.R., Gjerde, K.M., Kittinger, J.N., Friedlander, a. M., Gaines, S.D., Clark, M.R., Thurnherr, a. M., Hardy, S.M. & Crowder, L.B. (2015) Managing mining of the deep seabed. *Science*, **349**, 144–145.

Weinberg, C., Titschack, J., Freiwald, A., Frank, N., Lundälv, T,, Taviani, M., Beuck, L., Schröder-Ritzrau,, A., Krengel, T. & Hebbeln, D. (2018) The giant Mauritanian cold-water coral mound province: Oxygen control on coral mound formation. *Quaternary Science Reviews*,**185**,135-152.

Weir, B.S. & Cockerham, C.C. (1984) Estimating F-statistics for the analysis of population structure. *Evolution*, **38**, 1358–1370.

White, M., Mohn, C., Stigter, H. de, & Mottram, G. (2005) Deep-water coral development as a function of hydrodynamics and surface productivity around the submarine banks of the Rockall Trough, NE Atlantic. *Cold-water Corals and Ecosystems* (ed. by A. Freiwald and J.M. Roberts), pp. 503–514. Springer, Erlangen Earth Conference Series, Berlin, Heidelberg.

Widmer, A. & Lexer, C. (2001) Glacial refugia: Sanctuaries for allelic richness, but not for gene diversity. *Trends in Ecology and Evolution*, **16**, 267–269.

Wilson, A.B. & Eigenmann Veraguth, I. (2010) The impact of Pleistocene glaciation across the range of a widespread European coastal species. *Molecular Ecology*, **19**, 4535–4553.

Zahn, R., Schönfeld, J., Kudrass, H.R., Park, M.H., Erlenkeuser, H. & Grootes, P. (1997) Thermohaline instability in the North Atlantic during melt water events: Stable isotope and ice-rafted detritus records from core SO75-26KL, Portuguese margin. *Paleoceanography*, **12**, 696–710.

Zibrowius, H. (1980) *Les Scléractiniaires de la Méditerranée et de l'Atlantique nord-oriental*, Institut Oceanographique Fondation Albert 1er, Prince de Monaco.

xi. Biosketch

Ronan Becheler is a postdoctoral researcher in evolutionary ecology and population genetics. His research interests concern the evolutionary consequences of reproductive systems, with a special emphasis on partial clonality. He has worked on the assessment of dispersal in coastal and deep-sea species. Currently, he studies the evolution of reproductive strategies and local adaptation in temperate macroalgae.

Joana Boavida is a postdoctoral researcher interested in biodiversity-related disciplines, from taxonomy to biogeography and macroecology, typically using corals as model systems.

xii. Appendices

An appendix shows supporting information

xiii. Supporting information is supplied in a separate file

TABLE S1 - SUMMARY OF SAMPLING LOCATIONS

S2 - ADDITIONAL METHODS

S2.1 - CORE COLLECTION AND DATING

S2.2 - DNA AMPLIFICATION AND SEQUENCING

S2.3 - SPECIES DELIMITATION

S2.4 - GENETIC DIVERSITY AND PHYLOGEOGRAPHIC PATTERNS

S2.4.1 - Internal transcribed spacer (ITS) sequences

Figure S1 - Bayesian Skyline Plots.

S2.4.2 - Microsatellites

Figure S2 - Inference of the number of clusters in the DAPC

S2.5 - APPROXIMATE BAYESIAN COMPUTATION (ABC)

S2.5.1 - Specific model parameters and model checking procedure

Figure S3 - Approximate Bayesian Computation scenarios tested.

Figure S4 - Logistic regression of the posterior probabilities of the tested ABC demographic scenarios.

Table S2 - Estimated ABC parameters

FIGURE S5 - POWER ANALYSES

TABLE S3 PAIRWISE FST, BASED ON ITS HAPLOTYPIC FREQUENCIES

TABLE S4 - PAIRWISE FST, FOR MICROSATELLITE LOCI

TABLE S5 - ANALYSIS OF MOLECULAR VARIANCE (AMOVA) FOR MICROSATELLITES

TABLE S6 - ANALYSIS OF MOLECULAR VARIANCE (AMOVA) FOR ITS

TABLE S7 - FREQUENCY DISTRIBUTION OF ITS HAPLOTYPES

FIGURE S6 - STATISTICAL PARSIMONY NETWORK

FIGURE S7 - TESS CROSS-VALIDATION SCORE

FIGURE S8 - FIELD PICTURE OF FOSSILISED CORALS FROM CORE CS01

SUPPLEMENTARY PALEO-HISTORY

PALEO-HISTORY REFERENCES

ADDITIONAL REFERENCES

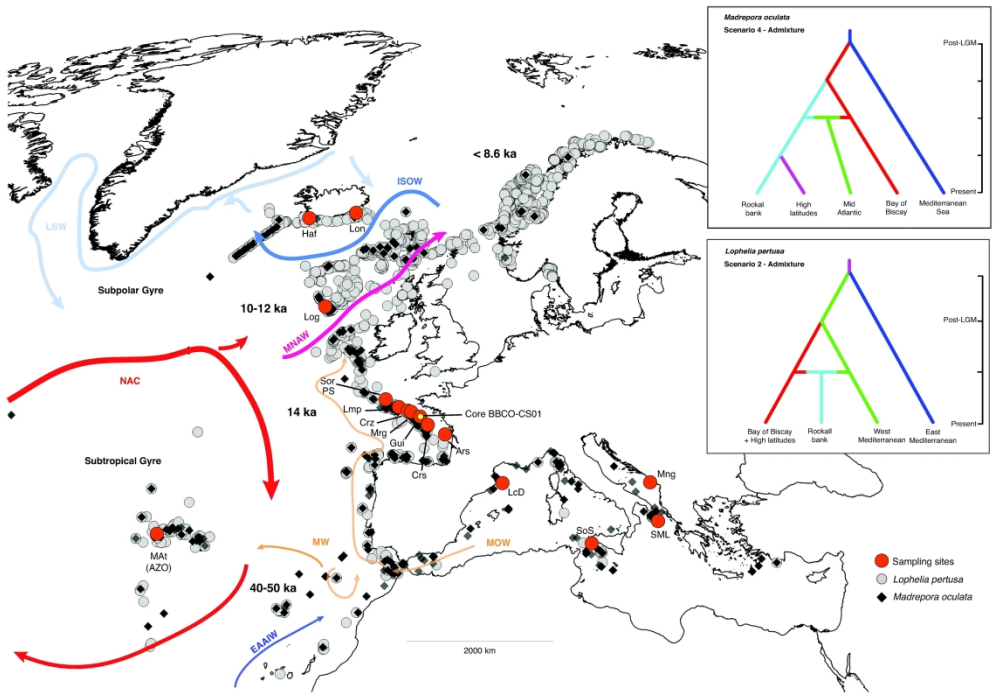

Figure 1 - . Contemporary distribution of M. oculata (black diamonds) and L. pertusa (grey circles) in the NE Atlantic, (2017 UNEP database; http://data.unep-wcmc.org) and the path of the main North East Atlantic Ocean currents (adapted from Montero-Serrano et al., 2011, Somoza et al., 2014 and Cossa et al., 2018): MOW - Mediterranean Outflow Water; MW - Mediterranean Sea Water; NAC - North Atlantic Water; MNAW - Modified North Atlantic Water; EAAIW - Eastern Antarctic Intermediate Water; LSW - Labrador Sea Water; ISOW - Iceland-Scotland Overflow Water. Site abbreviations as in Table 1. Dates correspond to estimated ages for coral mound growth (adapted from Schröder-Ritzrau et al., 2005). Insets are the selected demographic history models for each cold-water coral species. ka - thousand years ago. Map created on QGIS with Mollweide's equal area projection.

296x209mm (300 x 300 DPI)

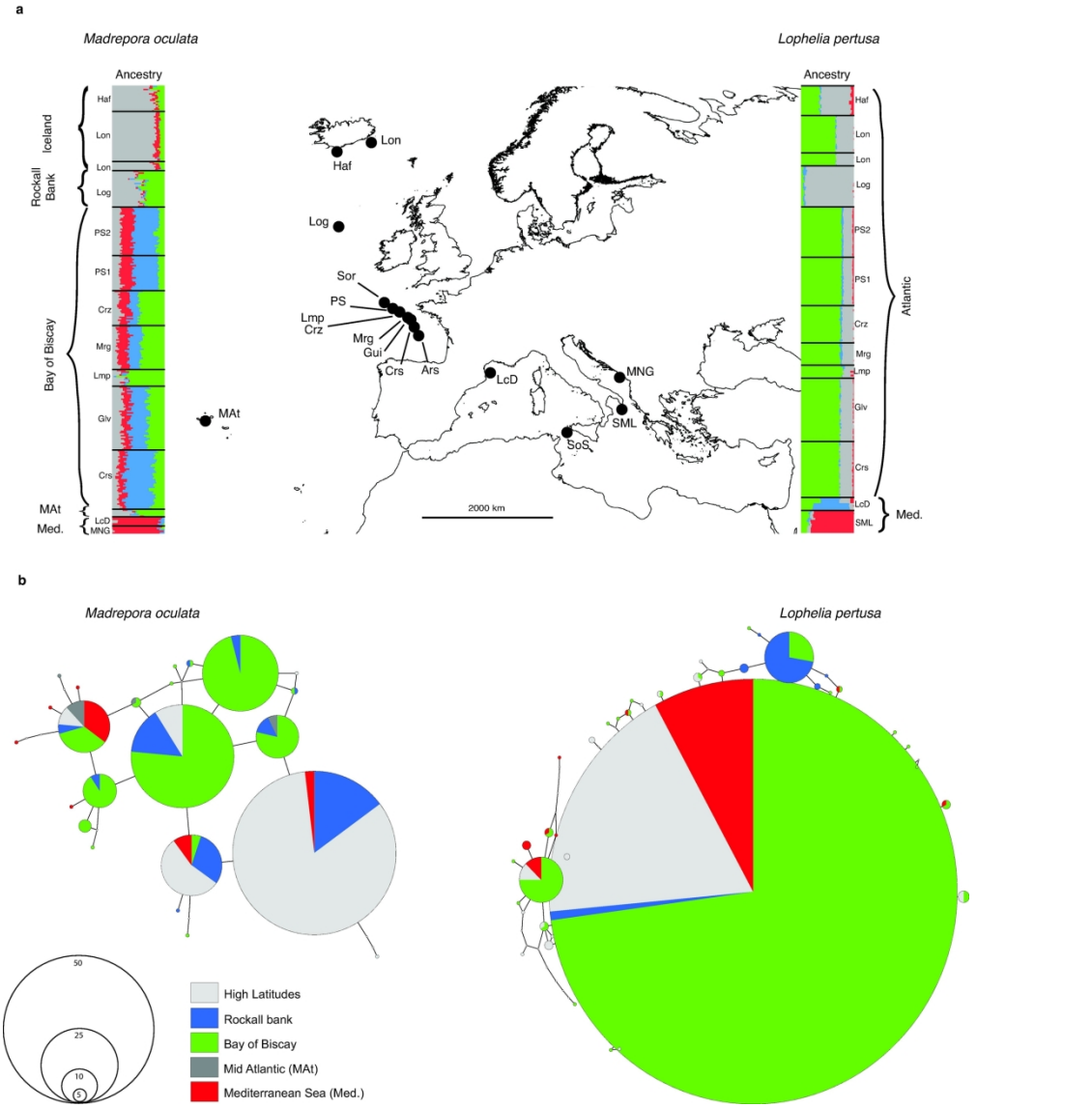

Figure 2 - Genetic subdivision among global regional samples. (a) Population membership diagrams displaying the probability of each individual into K K = = 4 clusters for Madrepora oculataMadrepora oculata (left) and K = 2 for Lophelia pertusaLophelia pertusa (right) (denoted by different colours). Each individual is depicted by a horizontal line partitioned into K coloured sections, with the length of each section proportional to the estimated membership ancestry coefficient proportion (Qind) to each cluster. Sample names refer to sites indicated in table and Fig. 1. Samples from the Bay of Biscay canyons (left diagram) are geographically ordered from north to south according to what is shown on Fig. 1. Black horizontal lines separate adjacent sites (MAt - Mid Atlantic, Med. - Mediterranean). The map shows the distribution of M. oculata (black diamonds) and L. pertusa (grey circles) known occurrences, according to the 2017 UNEP database (http://data.unep-wcmc.org). Map created on QGIS with GDAL bathymetry and the equal area Mollweide projection. (b) Parsimony haplotype networks based onof Internal Transcribed Spacer ribosomal sequences for M. oculataM. oculata (left) and L. pertusaL. pertusa (right). The size of the circle is proportional to the observed number of sequences for the corresponding haplotype. Pie charts illustrate the proportion of a haplotype found in each region. The length of links is proportional to the number of mutations separating two haplotypes; the shortest represent a single mutation. Mediterranean includes Ionian Seaeastern and western basin samples.

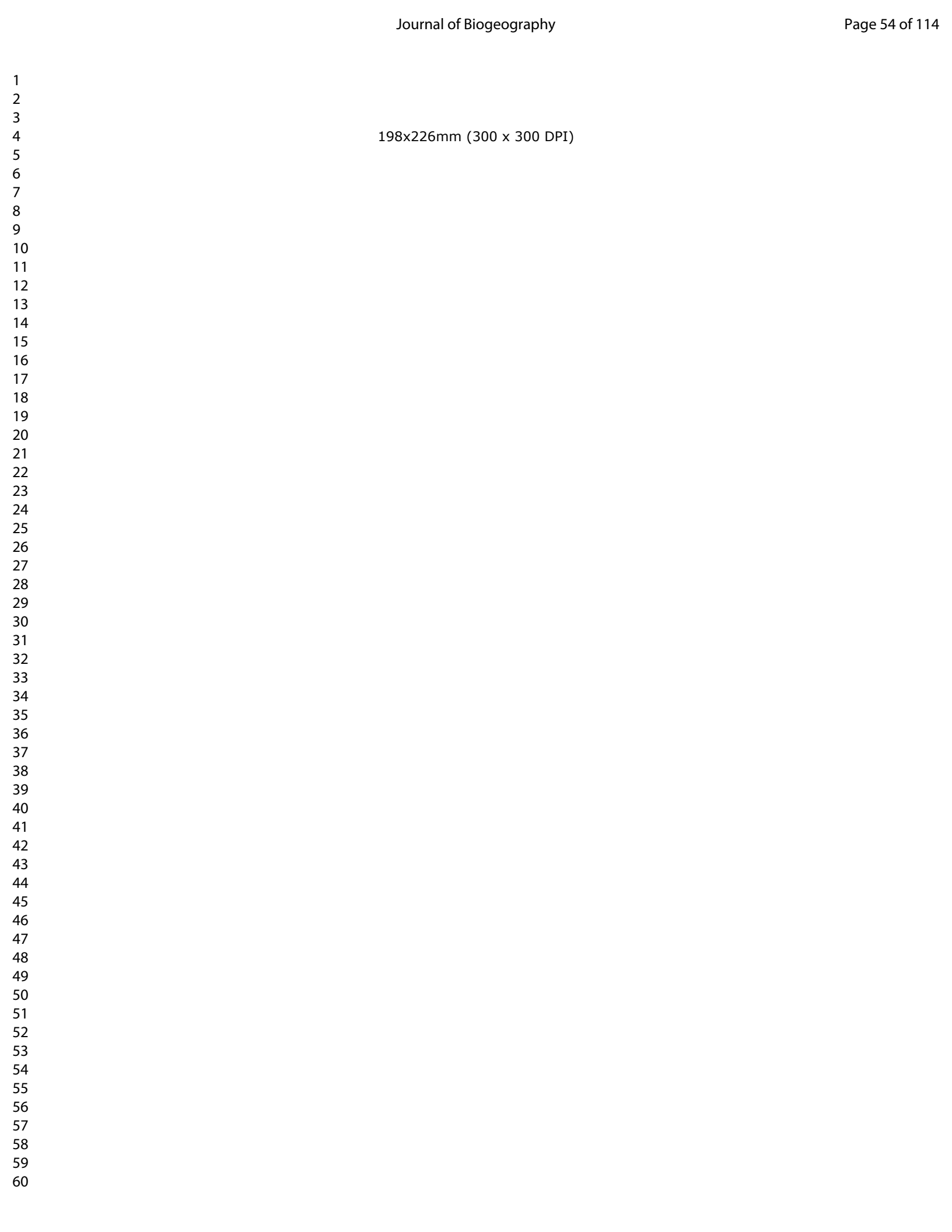
198x226mm (300 x 300 DPI)

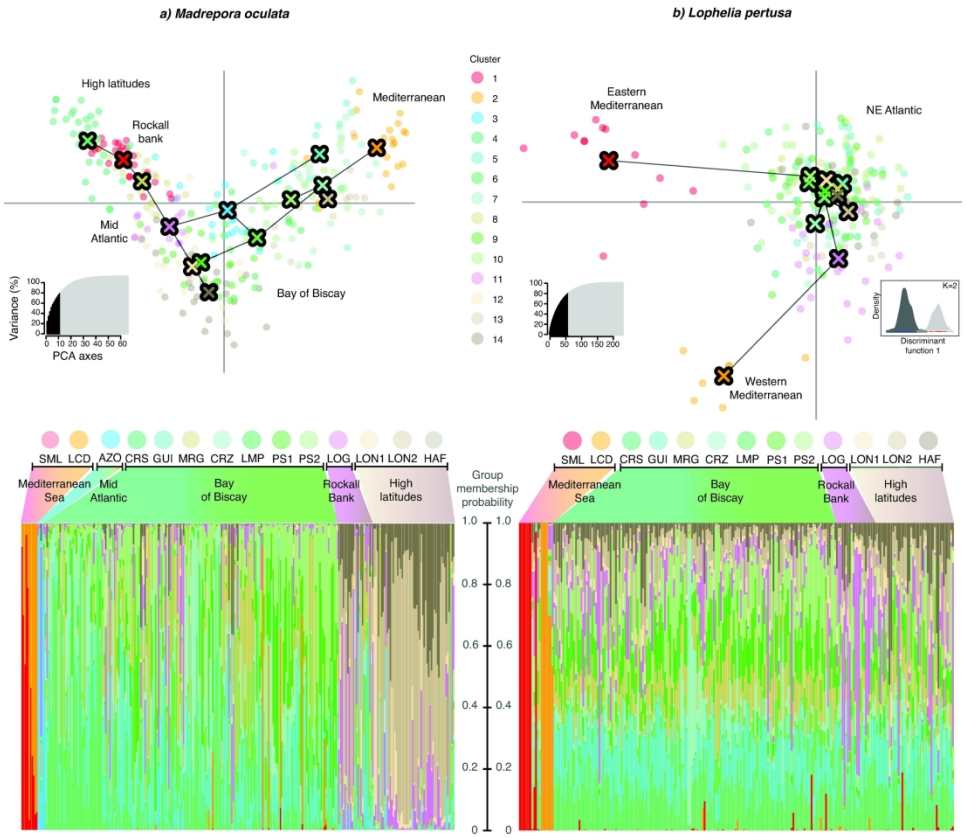

Figure 3 - Genetic subdivision among regional samples. Top - Discriminant Analyses of Principal Components (DAPC). A minimum-spanning tree based on the squared distances between groups connects group centres (crosses). Insets show the variance explained by the principal components included in the analyses (black). Because the identified optimal number of genetic clusters (K) for Lophelia pertusa is K=2 (see additional inset with sample density along the first discriminant function), the DAPC plot for L. pertusa shows samples color-coded by sampling site. Bottom - Population membership diagrams displaying the probability of each individual colour-coded by sampling site.

218x181mm (300 x 300 DPI)